HIGHLIGHTS

Valle di Manche—candidate Ionian GSSP (Middle Pleistocene)

Ostracod and mollusk respond in a synchronized manner to glacial-interglacial oscillations

Meiofaunal stratigraphic trends parallel oxygen isotope stratigraphy

Multivariate paleoecology: an effective tool for sequence stratigraphic interpretations

Response of ostracod and mollusk marine communities to Early-Middle Pleistocene environmental changes: the Valle di Manche stratigraphic record (GSSP candidate section, Southern Italy)

Veronica Rossi[1], Michele Azzarone[1], Luca Capraro[2], Costanza Faranda[3], Patrizia Ferretti[4], Patrizia Macrì[5], Daniele Scarponi[1]*

[1] Dipartimento di Scienze Biologiche, Geologiche e Ambientali, University of Bologna, via Selmi 3, I-40126 Bologna, Italy

[2] Dipartimento di Geoscienze, University of Padova, Via G. Gradenigo 6, I-35131 Padova, Italy

[3]Dipartimento di Scienze, University of Roma Tre, Largo San Leonardo Murialdo 1, 00146 Roma, Italy

[4]Consiglio Nazionale delle Ricerche, Istituto per la Dinmica dei Processi Ambientali (CNR-IDPA), Via Torino 155, I-30172, Venezia Mestre, Italy

[5]Istituto Nazionale di Geofisica e Vulcanologia, Via di Vigna Murata 605, I-00143 Roma, Italy

* corresponding author

Abstract

The Valle di Manche (VdM) section (Calabria, Southern Italy), is one of the candidates to host the Global Stratotype Section and Point of the Ionian Stage (Middle Pleistocene). It offers the opportunity to investigate the ostracod turnover along a continuous shelf succession straddling the Early-Middle Pleistocene boundary, and compare it against other paleoenvironmental (i.e., mollusks) and paleoclimatic (*Uvigerina peregrina* $\delta^{18}O$) records. High-resolution (ca. 1 sample/meter) ostracod fauna quantitative data, coupled with gradient analyses (Detrended Correspondence Analysis and nonmetric Multi-Dimensional Scaling), document a strong relationship between changes in faunal composition and lithofacies vertical stacking patterns. The comparison between the mollusk- and ostracod-derived ordination data demonstrates that the meio- and macro-faunal turnover are guided by a common complex gradient: bathymetry. The integrated ostracod-mollusk gradient analysis also provides trend in water depths along

the section, highlighting to what extent such multivariate approach can improve the paleoenvironmental and sequence stratigraphic interpretation of ancient shallow marine successions. When plotted stratigraphically, ordination major axis sample scores reveal two increasing-decreasing patterns in water paleo-depth that fit well with the T-R cycles previously identified. Paleobathymetric estimates combined with the vertical distribution of key ostracod groups (i.e., epiphytic taxa on sandy substrates vs. deep-sea mud lover taxa) allow refining depositional trends, stratal stacking patterns and position of previously not well resolved sequence stratigraphic surfaces within each T-R cycle (e.g., Transgressive Surface-TS). Indeed, two rapid increases in water depth values mark the TSs that separate shallowing-upward, progradational (RST) from deepening upward, retrogradational (TST) stratal stacking patterns of shelf deposits. The TSs, which underline fine-grained successions dominated by deep-sea mud lover taxa, are invariably constrained to the inception of interglacials MIS 21 and MIS 19, identified within the VdM section by benthic foraminifera $\delta^{18}O$ values. Within both the VdM T-R cycles, the deepest conditions (ca. 140 m of water depth) are invariably identified within the *Neopycnodonte* unit, slightly above of the lightest $\delta^{18}O$ intervals. The overlying decreasing bathymetric trend, coupled with shifts in ostracod ecological groups, allows to identify in the bryozoans lithofacies the stillstand+falling of the relative sea-level, also tracked by a progressively heavier $\delta^{18}O$ record. More stable paleobathymetric conditions (around 40-45 m of water depth) characterize the overlying silt-sand deposits dominated by epiphytic species and showing the heaviest $\delta^{18}O$ values.

Keywords: Stratigraphic Paleobiology; Ionian Stage; Ordination Analysis; Glacial-Interglacial Cycles

1. Introduction

During the last decades, the value of marine benthic fauna and related traces as paleoenvironmental and paleoclimatic proxy has been exploited in several Quaternary and pre-Quaternary successions (e.g. Murray, 2006; Baucon et al., 2012; Horne et al., 2012; Horton et al., 2013; Avila et al., 2015; Gliozzi et al., 2015; Huntley and Scarponi, 2015; Bruno et al., 2017). Specifically, the distribution of ostracods in almost every aquatic depositional settings and their good ecological sensitivity to changing environmental

conditions make these small crustaceans (0.4 to 2.0 mm on average) a routinely employed tool in paleoenvironmental reconstructions from continental to marine settings (e.g., Bonaduce et al., 1975; Henderson, 1990; Montenegro and Pugliese, 1996; Faranda et al., 2007; Pascual et al., 2008; Marriner and Morhange, 2007; Bini et al., 2012; Marco-Barba et al., 2013a,b; Grossi et al., 2015; Martínez-García et al., 2015; Mazzini et al., 2015, 2017). Recent studies have also documented the ostracod capability to track high-frequency and high-energy depositional events (paleofloods) in the marine realm (Angue Minto'o et al., 2015; Fanget et al., 2016). In contrast, minor attention has been paid on the relevance of marine ostracods in identifying stratal stacking patterns and depositional trends in a sequence stratigraphic perspective, also with respect to other biological proxies (e.g., Yasuhara et al., 2012; Amorosi et al., 2014a).

Through time, a series of Plio-Pleistocene open marine sections outcropping in Southern Italy, and considered of great significance for the chronostratigraphy of the Quaternary period (i.e., Monte San Nicola, Vrica, Montalbano Jonico and Fronte sections), were analyzed for the ostracod fauna to improve paleoenvironmental reconstructions (Colalongo and Pasini, 1980; Aiello et al., 2000, 2015; Amorosi et al., 2014b). Changes in paleobathymetry and dissolved oxygen/food availability are likely to represent the main drivers of the ostracod turnover in these sections (e.g., Marino et al., 2015; Negri et al., 2015). The Valle di Manche (VdM) section (Calabria, Southern Italy; Fig. 1A-B), a candidate to host the Global Stratotype Section and Point (GSSP) of the Ionian (Middle Pleistocene; Cita et al., 2006; Head and Gibbard, 2015), is currently lacking of a detailed ostracod investigation, notwithstanding its high potential.

The VdM section represents an ideal venue where to investigate the main driver(s) of ostracod turnover and test ostracods capacity of tracking environmental changes, as its tens m-thick succession of marine deposits is firmly constrained in time (Early-Middle Pleistocene transition; Rio et al., 1996; Fig. 1B). In addition, a quasi-continuous, high resolution record of benthic foraminifera $\delta^{18}O$ values ($\delta^{18}O$ *Uvigerina peregrina*) offers a well-defined framework of Milankovitch climate-eustatic variability (from late MIS 22 to early 18, Capraro et al., 2005; 2017). Lastly the reconstruction of macrobenthic turnover and derived paleobathymetric quantitative estimates (Scarponi et al., 2014) furnish the rare opportunity to compare ostracod dynamics against a different paleoecological proxy into a shelf setting. In this respect, distinct

benthic groups (i.e., mollusks and ostracods) may show differential response to the drivers of environmental change, because of differences in their ecological requirements.

The main purpose of this study is to describe the vertical distribution patterns of ostracods across the middle portion of the VdM section (Fig. 2) to *(i)* evaluate if ecologically different and widely used proxies as ostracods and mollusks show comparable turnover along the same sedimentary record or if they respond to different driver(s) of environmental change and *(ii)* highlight to what extent ostracod quantitative analyses can improve and refine the VdM stratigraphic and paleonvironmental framework (e.g., biofacies characterization and stratal stacking patterns), also in the view of its candidature as GSSP. Indeed, integrated investigations involving multiple environmental proxies have the greatest potential to increase our understanding of biotic responses to environmental changes, meanwhile allowing for a clearer reconstruction of the stratigraphic architecture of sedimentary successions (e.g., Amorosi et al., 2014a; Rossi et al., in press).

2. Geological setting

2.1 The Crotone Basin

The Crotone Basin (CB hereafter, Calabria, Southern Italy; Fig. 1A) is located above the internal part of the Calabrian accretionary wedge (Rossi and Sartori, 1981) and hosts a remarkably thick, well-exposed and highly fossiliferous succession, upper Miocene to Pleistocene in age. As the San Mauro Marchesato confined sub-basin, within the central sector of the CB (Fig. 1A), has been affected by high subsidence related to tectonic activity (see Van Dijk, 1994; Speranza et al., 2011; Macrì et al., 2014), marine sedimentation lasted till the Middle Pleistocene (Capraro et al., 2006; Massari et al., 2010). Within the investigated sub-basin, the upper tectono-stratigraphic unit (San Mauro Sandstone unit of Roda, 1964) was further subdivided (Rio *et al.*, 1996) into three sub-units (SM1 to SM3) that can be conveniently traced across the San Mauro sub-basin and in part across the VdM section (Fig. 1B).

The SM2 unit, ca. 5 to 40 m thick, spans from the uppermost MIS 22 to the full MIS 18.4 glacial (Capraro et al., 2005; 2017; Fig. 1B). It consists of greyish, prominent packages of marine deposits ranging from silty

muds to sandy silts, which reflect a series of deepening and shallowing trends between “fully glacial sand-packages” pertaining to MIS 24/22 and MIS 18. Indeed, stratal geometries of the SM2 point to a major increase in tectonic subsidence rates, which emphasized the glacioeustatic sea-level rise after the MIS 24/22 glaciation (Capraro et al., 2005). The overlying unit (SM3, Middle Pleistocene) is characterized by thick sandstone/conglomerate bodies showing a distinct shallowing-upward trend, predating the definitive uplift of the sub-basin, possibly occurred in the Middle Pleistocene (Capraro et al., 2011; Fig. 1B).

Hence, the San Mauro sub-basin is represented by a synsedimentary growth syncline that developed since the late Calabrian (Rio et al., 1996; Massari et al., 1999), where continuous creation of accommodation space allowed the deposition of a cyclothemic, shallowing-upward marine to continental succession (Fig. 1B), and the Valle di Manche section represents one of the best-preserved locations.

2.2 The Valle di Manche section

The investigated portion of the Valle di Manche (VdM) section straddles the Early-Middle Pleistocene transition (MIS 21 to early MIS 18) and is ca. 35 m-thick. Bio-, magnetostratigraphic proxies and $\delta^{18}O$ records invariably constrain the VdM muddy deposits to the interglacial periods (MIS 21 and MIS 19), whereas the coarser-grained successions developed under glacial (MIS 20 and MIS 18) conditions (Figs. 1B, 2). A prominent ash layer (“Pitagora Ash”), which approximates the Matuyama–Brunhes geomagnetic reversal (mid MIS 19), is recorded within the upper portion of VdM section (Figs. 1B, 2; Capraro et al., 2017). The sequence stratigraphic framework of VdM section can be roughly outlined on the basis of the sole sedimentary features, it contains two depositional units (cyclothems 6 and 7 in Massari et al., 2002; Figs. 1B, 2) interpreted as two transgressive-regressive (T-R) cycles (Capraro et al., 2017 and references therein). Indeed, each depositional cycle is composed of several lithofacies (Fig. 2), here briefly described (further details are available in Massari et al., 2007 and Capraro et. al., 2015).

Lithofacies A up to 4.5 m thick, is represented by dark, massive muds (mainly silty clays) that contains in its lower portion large dispersed burrows, vegetal remains and sulphide nodules. The macrofossils are very scarce but increase upwards, and are mainly represented by assemblages dominated by *Corbula gibba*. The latter is here indicative of hypoxic conditions (see also Ceregato et al., 2007).

Lithofacies B less than 1m thick, is composed of loosely packed macrofossil remains embedded in a matrix of mud (clayey silts). Clumps of the gregarious deep-sea ostreid *Neopycnodonte* along with unsorted, variable preserved shelly material are the most striking features of this lithofacies and are indicative of an ecologically condensed interval (see also Scarponi et al., 2014, 2017).

Lithofacies C several meters thick, is mainly represented by fine to coarse silts grouping a series of macrofossil rich units. It has been subdivided in three sub-lithofacies based on macrofossil remains and lithologic features (Capraro et al., 2017). C1: ca. 2.5 m-thick, is composed of amalgamated muddy-silts rich in bryozoans and others unsorted macrofossils (mainly small-sized mollusks). C2: up to 1.5 m-thick, consists of silts rich in bryozoans alternating to poorly fossiliferous clayey strata characterised by *Chondrites* (disaerobic fossil traces, Bromley and Ekdale, 1984). C3: up to 6 m-thick, massive silts containing dispersed skeletal material (mainly mollusks and bryozoans). Sparse vegetal remains and strings of the polychaeta *Ditrupa*, indicative of high sedimentation/turbidity and unstable mixed substrates along shelf (Cosentino and Giacobbe, 2006), increase in abundance upwards.

Lithofacies D is made up of ca. 8 m-thick succession of silts with sparse macrofaunal content, embedding cm-to-dm thick sharp based, densely laminated fine sands with abundant strings of plant debris. Coarser layers are locally interbedded with physical concentrations of disarticulated and oriented shells (mainly pectinids and polychaetes) indicative of high-energy events, such as river floods and/or storm-induced flows within shelf settings (Massari et al., 1999).

Lithofacies E is ca. 1 m-thick of loosely packed *Turritella tricarinata* shells within a silt matrix, retrieved only in the middle portion of the investigated section. *T. tricarinata* is considered a semi-infaunal filter feeder that attains high abundance in sandy muddy substrata subject to influence of riverine waters (Dominici, 2001).

3. Material and methods

3.1 Ostracod data collection

157 Recently, a high-resolution sampling campaign (ca. 20 cm/sample) has been performed for fossil and
158 geochemical analyses taking the “Pitagora Ash” as the reference zero level (Capraro et al., 2015; Fig. 2).
159 Following stratigraphic criteria, 39 samples have been chosen to undertake a high-resolution study of the
160 ostracod fauna across the VdM section and within each depositional sequence. Selected samples are 1
161 meter or less spaced apart from each other (Fig. 2); special attention (higher sampling resolution) is paid to
162 the muddy units and the fossiliferous silty intervals, where a rich ostracod fauna is expected.
163 Samples (ca. 50-55 g dry weight each) were soaked overnight in hydrogen peroxide solution (4% H_2O_2),
164 gently water-screened with a 63 µm-mesh sieve and dried in an oven at 40°C for 8 hours. Each sample
165 residue was qualitatively observed under a binocular microscope, described and split into small portions. If
166 possible at least 100-150 well-preserved ostracod valves were counted for each sample in the size fraction
167 >125 µm (carapace was counted as two valves), otherwise all valves retrieved were counted. The presence
168 of juveniles/young instars was noted, being a useful indicator of the autochthony along with the state of
169 preservation of valves (Boomer and Eisenhauer, 2002), but not considered for counting. Ostracod
170 specimens were mostly identified and counted at species level under a binocular microscope. Species/taxa
171 relative abundances (%) were also calculated for each sample, as well as the species diversity (fisher alpha
172 index on samples with n>10 valves; Bassetti et al., 2010).
173 The VdM dataset includes ~3650 valves, belonging to ca. 90 species, 38 genera and 3 groups (*Krithe*
174 spp., *Parakrithe* spp. and *Callistocythere* spp.). Fossil counts and relevant literature used for taxonomic
175 identification are reported in Supplementary Material (SOM-Appendix 1; Table S1). Less than 10% of the
176 encountered species are considered extinct. Furthermore, variable amounts of clearly allochthonous
177 specimens, showing evidences of transport (i.e., blackish colors, traces of abrasion and/or shell damages),
178 are also found. All the allochthonous specimens (mainly belonging to genera *Aurila*; *Callistocythere*;
179 *Carinocythereis*; *Costa*; *Loxoconcha*; *Limnocythere*; *Pontocythere*; *Pseudocandona* *Urocythereis*;
180 *Semicytherura*; *Krithe* and *Henryhowella*) were not inserted in the VdM ostracod dataset.
181 The relative abundances of a selection of taxa (i.e. the most common and/or informative in terms of
182 paleoenvironments) were stratigraphically plotted against the studied section. The structure and
183 composition of this representative portion of the ostracod fauna was described and interpreted with

184 respect to each lithofacies (Section 2.1), to define ostracod-lithofacies relationship and possibly refine
185 facies paleonvironmental characterization. The taxon relative abundance *vs*. stratigraphic depth includes a
186 total of 4 groups and 14 species one of which, i.e. *Cimbaurila cimbaeformis*, is considered extinct in the
187 Calabrian (Faranda and Gliozzi, 2008). Groups include species belonging to the same genus and sharing
188 common ecological features.

189 **3.2 Gradient analysis**

190 Multivariate ordination techniques are applied to investigate ostracod faunal turnover and main
191 controlling driver(s) in shelf depositional settings at the Early-Middle Pleistocene transition. Specifically,
192 Detrended Correspondence Analyses (DCA) and nonmetric Multi-Dimensional Scaling (nMDS) are both
193 used. These unconstrained posteriori ordination approaches are commonly employed with compositional
194 data to identify major gradients in faunal composition (e.g., Scarponi and Kowalewski, 2004; Dominici et al.,
195 2008; Gliozzi and Grossi, 2008; Ligios et al., 2008; Pascual et al., 2008; Ritter et al., 2013; Berlanger and
196 Garcia, 2014; Kowalewski et al., 2015; Laut et al., 2016; Scarponi et al., 2017). Here, only DCA results are
197 reported (nMDS outputs in Figs. S1A-B; S2A-B). Despite DCA multiple drawbacks (e.g., Beals 1984; Jackson
198 and Somers 1991; McCune and Grace 2002) and difficulties in interpreting higher order gradients (axis>1;
199 Bush and Brame, 2010), DCA has proved to be effective when distribution of taxa relates to strong
200 variations in controlling environmental variables (e.g., Wittmer et al., 2014), which is likely the case here at
201 least for mollusk samples previously investigated (Scarponi et al., 2014).

202 For ordination analyses, the species-level data-matrix includes only samples showing more than 20
203 specimens (34 samples) and species recorded in more than one sample (51 species; SOM-Appendix 1). As
204 for DCA, faunal counts were log-transformed to prevent most abundant species dominating the gradient.
205 Whereas, nMDS analysis is performed on Bray-Curtis distance on both absolute and relative abundance
206 matrix (Figs. S1-2). However, varying the taxon and sample thresholds yielded comparable results (Figs.
207 S3A-F; Table 2A).

208 In addition, DCA and nMDS inferred ostracod faunal turnover was compared with that derived by DCA
209 analyses of mollusk assemblages (see Scarponi et al., 2014) sampled from the same record by means of
210 linear correlation (DCA mollusk *vs*. ostracod DCA/nMDS axis 1 sample scores; Table S2B). To avoid that

environmental variables driving changes in molluscan and ostracod faunas could reflect mainly differences in the number of samples and their sampling resolution (i.e., samples 17 *vs.* 34 and average sampling resolution 2.2 *vs.* 1 m/sample, respectively), a reduced ostracod dataset comparable to the mollusk one (in sample size and sampling resolution), was compiled and DCA and nMDS run (results reported in Table S2A and Fig. S3E). Then, the ordination axis 1 ostracod sample scores correlated to the mollusk-derived DCA axis 1 output of Scarponi et al. (2014; Table S2B). It is important to note that both mollusk- and ostracod-derived DCA scores are based on samples taken in the same stratigraphic interval (average offset 0.2 m, Table S2A).

As substrate consistency is one of the main drivers of ostracod turnover (and also could be related to water depth changes), we also employed a correlation model to evaluate if grain size (% of sand in a sample) is a linear function of DCA sample scores (see Table S3).

3.3 Environmental interpretation of the ostracod data

The ostracod environmental characterization of VdM lithofacies and an approximate interpretation of the main driver(s) of faunal turnover along the section (DCA axis 1), relied upon the auto-ecological characteristics and the present-day spatial distribution patterns of marine ostracods in the Mediterranean Sea and North Atlantic areas (e.g., Bonaduce et al., 1975; Breman, 1975; Athersuch et al., 1989; Sciuto and Rosso, 2008; Angue Minto'o et al., 2013; Cabral and Loureiro, 2013; Frezza and Di Bella, 2015; Sciuto et al., 2015).

All the extant retrieved species have, to a good approximation, well-to fairly-known ecological features. However, the relationship existing between abundances of extant ostracod species and the major abiotic marine parameters, such as bathymetry, substrate granulometry, percentage of organic matter and dissolved oxygen, is far to be quantified or, especially for extinct species, poorly investigated. For the latter species (e.g., *A. cimbaeformis*, *Cytherella gibba* and *Cytherella robusta* among the most common in the VdM dataset) only indirect ecological inferences can be employed (Aiello et al., 2015). Hence, further paleoenvironmental information were provided by comparing our data with those recorded within other Mediterranean shelf successions of late Quaternary age (Barra, 1991; Faranda et al., 2007; Aiello et al.,

2012, 2015; Sciuto and Meli, 2015) and those obtained from macrobenthic samples previously collected along VdM (Scarponi et al., 2014).

4. Results

4.1. The ostracod content of VdM lithofacies

The structure and composition of the autochthonous ostracod fauna is here analyzed for the first time and framed in the context of the lithostratigraphic framework recently defined by Capraro et al. (2017; Figs. 2, 4). Recurring vertical stacking patterns of lithofacies (except for facies E), developed during consecutive interglacial-glacial periods (e.g., MIS 21-20 and MIS 19-18), are a characteristic trait of VdM section. For each of the retrieved lithofacies (see Section 2.1), a description of the most representative/abundant ostracod taxa is reported below along with the paleoenvironmental interpretation. Selected species are also illustrated (see Fig. 3).

4.1.1 Lithofacies A

Within this lithofacies (ca. -22.5 to -19 m and -2.5 to 2.25 m; Fig. 4) the ostracod fauna is variable in terms of species richness and abundance, reaching a minimum close to the tephra layer (less than 10 valves). *Henryhowella sarsii*, *Krithe*-group and *Cytheropteron* species, mainly *C. monoceros* and *C. ruggierii*, are the dominant taxa with abundances up to more than 30%. Highly variable percentages of *Palmoconcha subrugosa* (0-20%), *Bosquetina tarentina* (0-25%) occur. Rare and scattered valves of *Paracytherois mediterranea*, *Bairdia conformis* and *Cytherella vulgatella* (less than 10%) are also recorded. High percentages of *Argilloecia*-group or *Pterygocythereis coronata* (up to ca. 20%) occur within the middle-upper portion of the lithofacies of both 6 and 7 T-R cycle. Taxa presently recorded in infralittoral-upper-circalittoral environments are scarcely represented, except at the basal portion of both cycles where not negligible percentages (up to 14%) of *Aurila convexa*, *Semicytherura ruggierii*, *Leptocythere multipunctata* and *Callistocythere* species occur.

The occurrence of lower circalittoral-epibathyal species (e.g., *H. sarsii*, *C. monoceros*, *B. tarentina*, *P. coronata*, Fig. 3), exclusively recorded at water depths >60-70 m in the Adriatic Sea (Bonaduce et al., 1975),

indicates a bathymetry compatible with an outer shelf (e.g., between ca. 80-150 m). Variable amounts of *H. sarsii*, a species preferring abundant and newly produced food resources (Fig. 3; Sciuto and Rosso, 2008), reflect changeable conditions of food quality and availability. In particular, *H. sarsii* seems to be locally replaced by species of the opportunistic genus *Cytheropteron* that is able to tolerate elevated fluxes of old organic matter (Sciuto and Rosso, 2008). Moreover, in the middle-upper part, high values of the infaunal (*Krithe*)/epifaunal (*H. sarsii*+*Cytheropteron*) ratio concomitant with the occurrence or increase in relative abundances of taxa tolerant to xenoxic conditions (i.e., *Argilloecia*-group or *C. vulgatella*; Fig. 3), suggest lower levels of oxygenation (Whatley, 1990; Aiello et al., 2015). In contrast, the remarkable amounts of infralittoral/upper circalittoral taxa (i.e., *A. convexa*, *Callistocythere* spp., *L. multipunctata;* Fig. 3) recorded in the lowermost portion of lithofacies A are interpreted to reflect a gradual increase in water depth.

4.1.2 Lithofacies B

The thin lithofacies B (ca. -19 to -18.5 m and 2.25 to 3 m; Fig. 4) shows a low-diversified ostracod fauna dominated by *Krithe*-group (ca. 7-64%) and *H. sarsii* (ca. 12-18%), accompanied by lower amounts of *B. tarentina* (up to ca. 12%) and *C. monoceros* (< 10%). Notable percentages of *Argilloecia* species (ca. 15%) and *B. conformis* (up to 10%) are found only within the lower T-R cycle (cycle 6). Rare valve of *P. coronata* (<3%) also occur. Taxa commonly reported from the infralittoral/upper circalittoral settings (i.e., *Aurila*, *Callistocythere* and *Leptocythere* species) are almost absent, except for the sporadic occurrence of *A. convexa* (abundances 0-7%).

The dominance of species preferring water depths >60-70 m (e.g., *B. conformis* Fig. 3), and the absence or low percentages of infralittoral/upper circalittoral genera indicates deposition in an outer shelf environment. Despite the good preservation state of *A. convexa* shells, the local occurrence of this infralittoral-upper circalittoral species can be related to sea bottom currents displacing ostracods from shallower water depths.

4.1.3 Lithofacies C1

Within this lithofacies (ca. -18.5 to -16 m and 3 to 5 m; Fig. 4) the ostracod fauna is quite diversified and shows the occurrence of lower circalittoral-epibathyal taxa (i.e., *H. sarsii*, *C. monoceros*, *B. tarentina*, *B. conformis* and *Argilloecia* species), mainly concentrated in correspondence of the lower portion of this unit.

However, species preferring infralittoral-upper circalittoral settings (i.e., *A. convexa*, *S. ruggierii*, *Leptocythere multipunctata*; Fig. 3), here constitute a remarkable component of the ostracod fauna. In particular, these species show in both T-R cycles an upward increasing trend paralleled by a strong decrease in relative abundances of *Krithe*-group. *Palmoconcha subrugosa* and *S. ruggierii* occur as secondary taxa (<13%), while minor amounts of *Callistocythere* spp. (0-6.4%) are found.

The composition of the ostracod fauna points to an upper circalittoral setting, as a mid-shelf (ca. 50-80 m water-depth range), with a granular-cohesive (silt-clay) bottom according to the high amounts of species preferring mixed substrates (*A. convexa*, *S. versicolor* in Fig. 3, and *S. ruggierii*). The upward increase trend in infralittoral-upper circalittoral species, which progressively replaces *Krithe*-group as dominant taxa, is interpreted to reflect a decrease in paleobathymetry and, possibly, a concomitant increase in vegetation cover at the sea floor.

4.1.4 Lithofacies C2

Lithofacies C2 (ca. -16 to -15 m and 5 to 7 m; Fig. 4) shows an ostracod fauna dominated by *S. ruggierii* (ca. 9.8-37%) and *A. convexa* (ca. 9.8-20%), with the secondary occurrence of *L. multipunctata* (ca. 2-11.7%), *Callistocythere* (ca. 3-14%) and *Krithe* (ca. 1.7-12.7%) groups, and *C. monoceros* (3-7.5%). Variable percentages of *B. tarentina* (0-6.4%), *P. subrugosa* (0-8.8%) and *S. versicolor* (0-7.4%) are also found.

The dominance of species typical of upper circalittoral-infralittoral environments (i.e., *S. ruggierii*, *A. convexa*, *L. multipunctata* and *Callistocythere* spp.) along with the not negligible occurrence of taxa preferring water depths from the upper circalittoral zone downward (mainly *C. monoceros* and *B. tarentina;* Fig. 3) suggests a mid-shelf depositional setting. High percentages of epiphytic taxa, mainly *A. convexa* and *Callistocythere* species, indicate a dense vegetation cover at the bottom.

4.1.5 Lithofacies C3

Along this lithofacies (ca. -15 to -11.5 m and 7 to 13.5 m; Fig. 4) ostracods are generally scarce (less than 10 valves) and characterized by a variable species diversity. *Aurila convexa*, *S. ruggierii* and *Callistocythere* spp. are well-represented, with the secondary occurrence of *Krithe*-group that locally peaks (up to ca. 48%) within the T-R cycle 7, in concomitance of a slight increase of *B. tarentina*, *H. sarsii* and/or *Cytheropteron* species (relative abundances >4%). Generally, scattered valves of *P. subrugosa*, *C. vulgatella* and *Argilloecia*

317 species occur in the investigated interval, reaching in one sample from the uppermost portion a total
318 amount of ca. 38% (T-R cycle 7; Fig. 4).

319 The dominance of *S. ruggierii* and epiphytic taxa as *A. convexa* and *Callistocythere* spp., along with the
320 secondary occurrence of ostracods commonly recorded at water depths >60-70 m (above all the *Krithe*-
321 group; Bonaduce et al., 1975), points to a vegetated mid shelf setting. However, the low abundance values
322 and the highly variable species diversity of the ostracod fauna suggest unstable environmental conditions.
323 Specifically, the high-frequency turnover involving *A. convexa*+*S. ruggierii* and *Krithe*-group+other
324 circalittoral-bathyal species (mainly *B. tarentina*), recorded within the uppermost T-R cycle, possibly reflects
325 abrupt shifts in water depths sometimes paralleled by changes in bottom conditions. In this regard, the
326 temporary establishment of a more pelitic substrate and lower levels of oxygenation is locally tracked by
327 the high amounts of the opportunistic species *P. subrugosa* (Fig. 3), that prefers muddy substrate, and taxa
328 tolerant to xenoxic conditions (*C. vulgatella* and *Argilloecia*-group).

329 **4.1.6 Lithofacies D**

330 This lithofacies (ca. -24 to -22.5 m and -11.5 to -4 m; Fig. 4) commonly contains a rich ostracod fauna
331 showing a marked upward increase in abundance (from ~20 to ~100 valves) and species richness. The
332 ostracod fauna is almost exclusively composed of typical infralittoral-upper circalittoral genera (i.e., *Aurila*,
333 *Callistocythere*, *Semicytherura* and *Leptocythere*) with the dominance of *Aurila-Cimbaurila* species (up to
334 33%), mainly represented by *A. convexa* and *C. cimbaeformis*. The latter is an extinct species (Early
335 Pliocene-Calabrian; Faranda and Gliozzi, 2008). Within the T-R cycle 6, *Leptocythere multipunctata* displays
336 an upward decreasing trend. A similar trend is also showed by *P. subrugosa*, *C. ruggierii* and *Krithe*-group
337 that are encountered with low percentages (commonly less than 8%). Rare displaced valves of freshwater-
338 low brackish ostracods belonging to genera *Limnocythere* and *Pseudocandona* are locally found.

339 The ostracod fauna structure (high species diversity) and composition (i.e., dominance of infralittoral
340 species along with absence/scarcity of species typical of lower circalittoral or deeper water species)
341 indicate an inner-mid shelf environment with silty-sandy bottoms covered by vegetation. The upward
342 decreasing trend of opportunistic taxa preferring muddy substrates (mainly *L. multipunctata*, *P. subrugosa*
343 and *Krithe*-group) reasonably reflects the progressive establishment of coarser bottoms and, shallower and

more stable environmental conditions according to the increase in species diversity. The local occurrence of few freshwater-low brackish ostracods fits with a shallow marine environment occasionally influenced by river fluxes.

4.1.7 Lithofacies E

Only one sample was analyzed for this lithofacies (-4 to -2.5 m; Fig. 4). It contains an ostracod fauna characterized by high amounts of *S. ruggierii* (ca. 23.5%) and *C. ruggierii* (ca. 12.5%), that is the only *Cytheropteron* species found. *Callistocythere* and *Krithe* groups occur with percentages less than 10%. Rare to very rare valves of *C. vulgatella*, *P. coronata*, *S. versicolor*, *P. subrugosa*, *P. mediterranea*, *H. sarsii* and *Argilloecia* spp. are also found. *Aurila* species are not recorded.

The occurrence of one species of *Cytheropteron* (*C. ruggierii;* Fig. 3), the only not rare in the Mediterranean infralittoral zone (Bonaduce et al., 1976; Aiello et al., 2015), and the very low amounts of taxa presently recorded at water depths deeper than 60-70 m (i.e., *H. sarsii* and *Argilloecia* spp.; Bonaduce et al., 1975) point to a depositional setting compatible with the upper (?) mid shelf.

4.2. *Indirect gradient analysis of VdM ostracod fauna*

The application of DCA (and nMDS) to the VdM ostracod dataset (34 samples and 51 species; SOM-Appendix 1), reveals a continuous distribution of both species and samples along the major axis of variation (DCA 1 Fig. 5; Fig. S1A,B; Table S2A). The effective occurrence of a strong environmental gradient underlying the major axis of variation is strengthened by the fact that both nMDS and DCA ordinations returned comparable results, while varying the taxon and sample thresholds (Figs. S2-3). In contrast, DCA axis 2 (DC2) is not easily interpretable as no evident relationship with any discernible physical-chemical variable related to ostracod ecology has been recognized.

The faunal turnover expressed along the major axis of variation (i.e., DCA1) can be associated with bathymetry, a complex gradient commonly retained to drive macrofaunal turnover in Quaternary or older marine successions (e.g., Scarponi and Kowalewski, 2007; Ayoub-Hannaa et al., 2013; Tyler and Kowalewski, 2014; Danise and Holland, 2017). Indeed, the position of several key ostracod extant species (highlighted in Fig. 5 and illustrated in Fig. 3), follows a positive bathymetric gradient from the left (DC1 low

scores) to the right (DC1 high scores) side of the axis of major variation. In particular, species typically found in infralittoral environments (e.g., *Aurila prasina*; *Hiltermannicythere rubra*) and infralittoral-upper circalittoral species reaching their highest abundances at water depths <50-70 m (e.g., *Aurila convexa*; *Pontocythere turbida*; *Leptocythere bacescoi*; *Leptocythere multipunctata*; *Leptocythere ramosa*; *Semicytherura incongruens*) plot on the left extremity of DC1 (DC1<50). Deep-sea species (lower circalittoral-epibathyal; >100m depth) e.g., *Henryhowella sarsii*; *Bosquetina tarentina*; *Baidia conformis* assemble on the far-right side (DC1>240). Whereas, in the middle DC1 portion (between 140-240), circalittoral taxa occur. Only two species presently abundant in shallow waters (i.e., *Microxestoleberis nana* and *Hemicytherura defiorei* in Fig. 5) attain high DC1 scores (deeper environments). This mismatch between present-day preferred bathymetry and DC1 scores of these two scattered species possibly indicates reworking in deeper setting.

The VdM samples also distributes along DC1 to the lithofacies supposed position along an onshore-offshore gradient (Fig. 5). Samples collected from the silt-sandy silt lithofacies D and C3 cluster (orange and yellow squares in Fig. 5) mainly locate on the left side (lower DC1 values). Moving toward higher DC1 values, samples collected from the fossil-rich shelf lithofacies (e.g., C1 and C2 showed in Fig. 5 as dark and light green squares, respectively) firstly occur followed by samples belonging to the deep-sea muddy lithofacies (A and B; dark and light blue squares in Fig. 5). However, the weak and not significant linear correlation ($r = -0.29$ $p = 0.09$) between sample granulometry and DCA1 sample score (Table S3B) suggest that substrate is not a strong driving factor of ostracod turnover along VdM section at this spatial and temporal scale of observation.

5. Discussion

5.1. Common causative factors drive ostracod and mollusk faunal turnover along the VdM section

The availability of both meiofaunal and macrofaunal censuses from the same lithofacies of the VdM succession offers the greatest potential for evaluating if such widely used biological proxy respond in a comparable manner to environmental drivers during two consecutive glacial-interglacial cycles.

The tight linear correlation between the first DCA axis 1 sample score of mollusk (from Scarponi et al., 2014) and DCA-1 ostracod dataset ($r^2 = 0.80$ $p < 0.001$; Table S2B) indicates a strong relationships between the faunal turnover of the two investigated ecological groups along the VdM succession. Similarly, this correlation holds also when the ostracod dataset is culled to be more similar, in terms of sample size and sample spacing, to the molluscan one ($r^2 = 20.78$ $p < 0.001$) and also when nMDS technique is employed (see Table S2B for correlation values). Hence, correlation analyses of meio- and macrofaunal censuses support the hypothesis that much of the variation in community composition (faunal turnover) recorded across the VdM lithofacies, which cover a wide spectrum of shelf depositional settings (Figs. 3, 4; Section 4), is tied to a common causative factor.

Recently published studies focused on the estimation of differences in the environmental drivers for ostracods *vs.* foraminifers (Yasuhara et al., 2012) and mollusks *vs.* foraminifers (Belanger and Garcia, 2014) in marine depositional settings. Quantitative inferences obtained in these studies suggested that foraminifers are sensitive to different environmental conditions compared to the other groups, reinforcing the supposition that both mollusk and ostracod faunas could be associable to the same drivers of community composition, especially when analyzed along a substantial portion of the marine gradient (i.e., entire shelf). However, to our knowledge, our reconstruction at VdM is one of the few studies specifically dealing with macro- and meiofaunal response to environmental drivers in open marine settings.

This redundancy should not be viewed as unfavorable to integrated analyses of ostracods and mollusks. On the contrary, the VdM results strengthen the high value of these faunal groups as paleoenvironmental tools, which may substitute each other or/and balance each other's weaknesses, especially considering that paleobiological data are strongly influenced by the stratigraphic framework. Indeed, the distribution of taxa along sedimentary successions is controlled not only by ecological processes (e.g., taxa environmental niches), but also (and equally important) by the sedimentary processes that govern whether fossil-containing sediments are deposited and preserved.

5.2 Drivers of macro and meiofaunal composition

421 The joint consideration of macro- and meiofaunal associations from the VdM section highlighted a
422 common cause driving faunal turnover along the section. Furthermore, the available ecological information
423 on ostracods coupled with the already investigated molluscan main drivers of faunal turnover, explored in a
424 companion paper (Scarponi et al., 2014), suggest that the majority of environmental variation could be
425 attributed to bathymetry (Fig. 5 and Section 4.2), and correlated environmental parameters.
426 In marine depositional contexts, bathymetry is a well-known indirect driver of macrofaunal turnover
427 (e.g., Tyler and Kowalewski, 2014) and in the fossil record bathymetry commonly shows the highest
428 correlation with faunal turnover (Patzkowsky and Holland, 2012; Wittmer et al., 2014, Scarponi et al.,
429 2017). This is especially evident when, as in this case, the sedimentary succession records
430 glacial/interglacial cycles developed along the entire shelf (Rio et al., 1996; Capraro et al., 2017).
431 On the other hand, the assessment and evaluation of the relative weights of the environmental
432 variables linked to the shelf bathymetric gradient, and potentially driving biotic response to environmental
433 change should require a wide set of measurements not yet available. Nevertheless, such highly interrelated
434 variations are here hinted by ecology information of ostracod taxa (Figs. 4, 6).
435 Given the coarse bathymetric information on ostracods taxa here recovered, water-depth calibrations of
436 unconstrained ordinations of ostracod samples (DCA1) rely on the rich amount of quantitative information
437 on bathymetry preference available for the majority of the mollusk species retrieved in concomitance or
438 proximity of sampled horizons (see Table S2A). Given the non-perfect concordance between the two sets of
439 sampling schemes (i.e mollusks *vs.* ostracods), reduced major axis regression of mollusk-derived
440 bathymetric estimates of samples *vs.* ostracods DCA 1 sample scores, allowed a rough calibration of
441 bathymetric ostracod samples (Table S4) and, more importantly, derived trends along the section (Fig. 6).
442 **5.3. Paleoenvironmental and sequence stratigraphic implications of the VdM faunal patterns**
443 The ostracod-mollusk faunal turnover recorded by DC1 sample scores outlines two similar v-shaped
444 patterns of variation that reflects two increasing-decreasing patterns in water depth and attributed to two
445 consecutive interglacial-glacial cycles on the basis of oxygen isotopic ratios (Fig. 6; MIS 21-MIS 18). Ecology
446 information on key taxa show also how changes in substrate conditions (lithology, vegetation cover and
447 oxygen/food type availability) are relatable to water depth inferences. Indeed, open marine ostracods

preferring muddy substrates (i.e., *H. sarsii*, *C. monoceros* and *Paracytherois mediterranea*) and species commonly recorded on vegetated sandy bottoms (i.e. *Aurila* and *Callistocythere* species) show, respectively, concordant and specular stratigraphic variation respect to DC1 sample score (Fig. 6). Thus, changes in substrate conditions (i.e. lithology and vegetation cover) tracked by the ostracod fauna are strictly connected to water depth inferences. In contrast, the temporary establishment of a stressed environment recorded by peaks in opportunistic species, tolerant to low oxygen levels (i.e. *Palmoconcha subrugosa*, *Palmoconcha turbida*, *Cytherella vulgatella* and *Argilloecia*-group), appears less clearly predictable in respect to water depth variations.

In the lowermost portion of the VdM section (ca. 24-19 m below the Pitagora Ash; Fig. 6), at the transition between lithofacies D-A, the abrupt upward increase in DC1 scores is paralleled by a marked shift towards lighter oxygen isotopic ratio, testifying the occurrence of a distinct bathymetric change during the interglacial MIS 21 (Fig. 6). Specifically, within the 3-meter-thick interval of muddy deposits (lithofacies A) the ostracod water-depth estimates record a steady deepening (from ca. 60 m to ca. 120 m; Fig. 6). The onset of this fast deepening upward trend, retrieved in proximity of decimetric thick sandy beds containing the boreal guest *A. islandica* (Scarponi et al., 2014), is retained to represent the transgressive surface (TS) separating the forced regressive/lowstand coarse deposits attributed to MIS 22 (estimated paleodepth ca. 50 m in the lower portion of the studied section, which possibly does not record the full glacial conditions but the following glacial termination; Fig. 6), from the overlying increasingly finer succession of MIS 21 age (Fig. 6). The retrogradational stacking pattern of facies, commonly characterizing transgressive successions (TST in Fig. 6), is also highlighted by the dominance of deep-sea (>70 m) mud-lover species, which depicts a coupled change in water depth and substrate lithology in respect to the underlying inner-middle shelf setting with vegetated coarser grained bottoms (lithofacies D; Section 4.1.6). Moreover, changeable conditions in terms of oxygen availability likely occur (lithofacies A; Section 4.1.1.) as testified by local peaks in opportunistic taxa (hypoxic conditions in Fig. 6).

Up section, the turnaround point of DC1 scores is recorded in correspondence of the *Neopycnodonte* unit (lithofacies B), where the maximum estimates of water depth are obtained (i.e. ca. 140m; Table S4) slightly above the lightest oxygen isotopic ratios (Fig. 6). Thus, based on coupled macro- and meiobenthic

475 inferences, lithofacies B is considered to represent the maximum flooding zone (MFZ) developed during the
476 MIS 21 interglacial peak (Fig. 6). Although no distinctive sedimentological features of the maximum flooding
477 surface (MFS) can be identified within unit B, an evident seaward shift of facies is here highlighted by the
478 initially gradual and then abrupt drop in DC1 scores recorded at the onset of the bryozoans-rich silt
479 deposits (lithofacies C1). The decreasing trend in DCA sample score reflects a rapid and continuous
480 decrease in bathymetry (from ca. 120 m to ca. 55 m; Fig. 6, Table S4) occurred during the glacial period MIS
481 20, as testified by the concomitant shift toward heavier values of $\delta^{18}O$ (Fig. 6). The re-establishment of
482 progressively shallower mid-shelf conditions during the MIS 20 sea level fall is clearly tracked also by the
483 abrupt diffusion of epiphytic taxa preferring sandy substrates to the detriment of deep-sea mud lover
484 species (Fig. 6). According to the development of a shelf vegetated sandy bottom, opportunist species show
485 an overall upward decreasing trend (Fig. 6).

486 Although the presence of a scarce ostracod fauna prevents a continuous record of DC1 scores across the
487 overlying silty-sandy deposits (lithofacies C3 and D), a relatively stable lowstand paleobathymetry can be
488 identified during fully glacial conditions of MIS 20 (heaviest values of $\delta^{18}O$ in Fig. 6). A minimum of water
489 paleodepth is reached close to the upper boundary of lithofacies D, where mud-lower species are almost
490 absent (Fig. 6).

491 The overlying *Turritella*-rich finer deposits/lithofacies E record a renewed slightly increase in deep-sea
492 species, paralleled by a sudden fall of epiphytic taxa (Fig. 6). This turnover in ostracod fauna composition is
493 clearly revealed by an abrupt increase in DC1 score values and tracks a rapid water-depth shift (~50 m to
494 ~80 m within 0.5 m of stratigraphic thickness), attributed to the MIS 19 transgression (upward lighter trend
495 in oxygen isotopic ratios; Fig. 6). This rapid and steady deepening trend is responsible for the subsequent
496 re-establishment of an outer shelf environment with muddy substrates (high amounts of mud-lover taxa)
497 and changeable oxygen conditions suggested by peaks in opportunistic species in the middle portion of
498 lithofacies A (Fig. 6). Hence, the lithofacies E lower boundary is marked by a shift from coarsening- and
499 shallowing-upward trend (i.e., coupled litho- and bio-facies C1-D) to a fining-and deepening-upward
500 succession (i.e., lithofacies E-A; Fig. 6). This shift from progradational to retrogradational stacking patterns
501 is interpreted to mark the transgressive surface (TS linked to MIS 19 interglacial; Fig. 6).

Thus, with respect to previously defined sequence stratigraphic interpretation (Fig. 2; Scarponi et al., 2014), the transgressive surface separating sequence 6 to 7, is here positioned at ca. -4 m. (Fig. 6), thanks to a higher resolution sampling scheme. As for the precedent depositional cycle attributed to MIS 21-MIS 20, ostracod fauna variations clearly trace an increasing-decreasing bathymetric trend with the turnaround point recorded within the upper portion of the *Neopycnodonte* unit, containing the MFS (water-depth estimate of ca. 140 m), to the overlying bryozoans deposits (lithofacies C1 and C2). The latter are constrained to the glacial MIS 18 by the $\delta^{18}O$ values trend (Fig. 6).

Integrated standard and ordination analyses of ostracod fauna also highlight the superposition of higher frequency changes on the overall shallowing-upward trend recorded within the lithofacies C3 of MIS 18 age (Fig. 6). One out of two main peaks in DC1 scores (at ca. 9 m and 13 m) matches with an increase in deep-sea mud lover species reinforcing the hypothesis of small-scale deepening pulsations (in the range of tens meters). However, at this resolution scale, we cannot totally exclude the influence of other factors, as upwelling currents. Comparable conditions have been identified by ostracods within coeval (MIS 18) shelf deposits belonging to the Montalbano Jonico-MJ section (Aiello et al., 2015), and interpreted as the consequence of upwelling episodes, leading to the sporadic co-occurrence of “deep” and “shallow” autochthonous ostracod taxa. The development of unstable paleoenvironmental conditions during the glacial MIS 18 is also supported by the local occurrence within lithofacies C3 of high amounts in opportunistic taxa tolerant to low oxygen levels (Fig. 6).

6. Conclusions

The combined use of a high-resolution, multi-proxy (ostracods and mollusks) dataset and multivariate ordination techniques (DCA and nMDS) on the VdM section (Calabria, Southern Italy), a candidate Ionian GSSP, has proved to be a powerful tool for investigating the main controlling driver on meio- and macro-faunal turnover in past shelf settings. Pairwise, quantitative ostracod analysis have demonstrated to be able to identify, within a shelf succession deposited during two consecutive glacial-interglacial cycles, specific stratal stacking patterns and a refined paleonvironmental and sequence stratigraphic interpretation of the section.

529 The major outcomes of this study can be summarized as follows:

530 • Ordination analysis performed on the VdM ostracod dataset shows a distinct
531 environmental gradient underlying the faunal turnover. This complex gradient corresponds to
532 bathymetry and associated parameters (e.g. vegetation cover), as documented by the ecological
533 information available for key extant species. Ostracod and mollusk communities respond in a
534 synchronized and similar manner to the environmental changes occurred on the shelf during two
535 consecutive glacial-interglacial cycles, from MIS 21 to 18.

536 • The integrated, multivariate analysis of ostracods and mollusks furnish a high-resolution,
537 reliable estimation of the paleobathymetric trends recorded within the VdM section, allowing an
538 improved differentiation between system tracts and identification of sequence stratigraphic
539 surfaces. Respect to previous studies, here the two TSs which represent the cycle boundaries are
540 precisely constrained by a high-resolution sampling that depict two rapid increases in water depth
541 values at the inception of interglacials MIS 21 and MIS 19 identified within the VdM section by $\delta^{18}O$
542 values.

543 • The joint consideration of macro- and meiofaunal associations prove to have the greatest
544 potential for interpreting ancient shallow marine successions in a paleonvironmental-sequence
545 stratigraphic perspective, meanwhile examining the biological and sedimentary response of shelf
546 settings to glacio-eustatic oscillations.

547 **7. Acknowledgments**

548 This work was supported by the RFO 2016, University of Bologna, Italy (DS and VR).

549

550 **Online Content**: Source Data along with any additional Extended Data display items are available in the
551 online version of the paper; references unique to these sections appear only in the online paper.

552

553 **8. References**

554 Aiello, G., Barra, D., & Bonaduce, G. 2000. Systematics and biostratigraphy of the ostracoda of the Plio-
555 Pleistocene Monte S. Nicola section (Gela, Sicily). Bollettino-Società Paleontologica Italiana, 39(1), 83-112.
556 Aiello, G., Barra, D., De Pippo, T., & Donadio, C. 2012. Pleistocene Foraminiferida and Ostracoda from the
557 Island of Procida (Bay of Naples, Italy). *Bollettino della Società Paleontologica Italiana*, 51(1), 50.
558 Aiello, G., Barra, D., & Parisi, R. 2015. Lower–Middle Pleistocene ostracod assemblages from the
559 Montalbano Jonico section (Basilicata, Southern Italy). *Quaternary International*, 383, 47-73.
560 Amorosi, A., Rossi, V., Scarponi, D., Vaiani, S.C., Ghosh, A., 2014a. Biosedimentary record of postglacial
561 coastal dynamics: high-resolution sequence stratigraphy from the northern Tuscan coast (Italy). Boreas 43,
562 939–954.
563 Amorosi, A., Antonioli, F., Bertini, A., Marabini, S., Mastronuzzi, G., Montagna, P., Negri, A., Rossi, V.,
564 Scarponi, D., Taviani, M., Angeletti, L., Piva, A., Vai, G.B., 2014b. The Middle-Upper Pleistocene Fronte
565 section (Taranto, Italy): an exceptionally preserved marine record of the last interglacial. Global and
566 Planetary Change, 119, 23-38.
567 Angue Mint'oo, C. A., Bassetti, M. A., Jouet, G., & Toucanne, S., 2013. Distribution of modern ostracoda and
568 benthic foraminifera from the Golo margin (East-Corsica). Revue de Paléobiologie, 32(2), 607-628.
569 Angue Minto'o, C. A., Bassetti, M. A., Morigi, C., Ducassou, E., Toucanne, S., Jouet, G., & Mulder, T., 2015.
570 Levantine intermediate water hydrodynamic and bottom water ventilation in the northern Tyrrhenian Sea
571 over the past 56,000 years: New insights from benthic foraminifera and ostracods. Quaternary
572 International, 357, 295-313.
573 Athersuch, J., Horne, D. J., & Whittaker, J. E., 1989. *Marine and brackish water ostracods* (superfamilies
574 *Cypridacea* and *Cytheracea):* keys and notes for the identification of the species (Vol. 43). Brill Archive.
575 Ávila, S.P., Ramalho, R.S., Habermann, J.M., Quartau, R., Kroh, A., Berning, B., Johnson, M., Kirby, M.X.,
576 Zanon, V., Titschack, J., Goss, A., Rebelo, A.C., Melo, C., Madeira, P., Cordeiro, R., Meireles, R., Bagaço, L.,
577 Hipólito, A., Uchman, A., da Silva, C.M., Cachão, M., Madeira, J., 2015 Palaeoecology, taphonomy, and
578 preservation of a lower Pliocene shell bed (coquina) from a volcanic oceanic island (Santa Maria Island,
579 Azores). Palaeogeography, Palaeoclimatology, Palaeoecology, 430, 57-73

580 Ayoub-Hannaa, W., Huntley, J. W., & Fürsich, F. T. 2013. Significance of Detrended Correspondence Analysis
581 (DCA) in palaeoecology and biostratigraphy: A case study from the Upper Cretaceous of Egypt. Journal of
582 African Earth Sciences, 80, 48-59.

583 Barra D. (1991). Studio del Pleistocene superiore-Olocene delle aree vulcaniche campane. Tesi dottorato
584 (*unpublished*) Università degli Studi di Napoli "Federico II", 298 pp.

585 Bassetti, M. A., Carbonel, P., Sierro, F. J., Perez-Folgado, M., Jouët, G., & Berné, S. 2010. Response of
586 ostracods to abrupt climate changes in the Western Mediterranean (Gulf of Lions) during the last
587 30kyr. *Marine* Micropaleontology, 77(1), 1-14.

588 Baucon, A., Bordy, E., Brustur, T., Buatois, L.A., De, C., Duffin, C., Felletti, F., Lockley, M., Lowe, P., Mayor,
589 A., Mayoral, E., Muttoni, G., Carvalho, C.N. De, Santos, A., Seike, K., Song, H., Turner, S., 2012. A History of
590 Ideas in Ichnology, in: Knaust, D., Bromley, R.G. (Eds.), Trace Fossils as Indicators of Sedimentary
591 Environments. Developments in Sedimentology 64. Elsevier, Amsterdam, pp. 3–43. doi:10.1016/B978-0-
592 444-53813-0.00001-0
593 Beals, E. W., 1984. Bray-Curtis ordination: an effective strategy for analysis of multivariate ecological
594 data. Advances in Ecological Research, 14, 1-55.

595 Belanger, C. L. & Garcia M. V., 2014. Differential drivers of benthic foraminiferal and molluscan community
596 composition from a multivariate record of early Miocene environmental change. Paleobiology, 40(3), 398–
597 416.

598 Bini, M., Brückner, H., Chelli, A., Pappalardo, M., Da Prato, S., & Gervasini, L., 2012. Palaeogeographies of
599 the Magra Valley coastal plain to constrain the location of the Roman harbour of Luna (NW
600 Italy). Palaeogeography, Palaeoclimatology, Palaeoecology, 337, 37-51.
601 Boomer, I., & Eisenhauer, G., 2002. Ostracod faunas as palaeoenvironmental indicators in marginal marine
602 environments. The Ostracoda: applications in Quaternary research, 135-149.
603 Boomer, I., Horne, D. J., & Slipper, I. J., 2003. The use of ostracods in palaeoenvironmental studies, or what
604 can you do with an ostracod shell. Paleontological Society Papers, 9, 153-180.

605 Bonaduce, G., Stazione zoologica (Napoli), Ciampo, G., & Masoli, M., 1975. Distribution of ostracoda in the
606 Adriatic Sea. LS Olschki; Taylor and Francis.
607 Breman, E., 1975. The distribution of ostracodes in the bottom sediments of the Adriatic Sea. Vrije
608 Universiteit van Amsterdam.
609 Bromley, R. G., & Ekdale, A. A., 1984. Chondrites: a trace fossil indicator of anoxia in
610 sediments. Science, 224, 872-875.
611 Bruno, L., Bohacs, K. M., Campo, B., Drexler, T. M., Rossi, V., Sammartino, I., Scarponi D., Hong, W.,
612 Amorosi, A., 2017. Early Holocene transgressive palaeogeography in the Po coastal plain (Northern Italy).
613 Sedimentology.
614 Bush, A. M., & Brame, R. I., 2010. Multiple paleoecological controls on the composition of marine fossil
615 assemblages from the Frasnian (Late Devonian) of Virginia, with a comparison of ordination
616 methods. Paleobiology, 36(4), 573-591.
617 Cabral, M. C., Loureiro, I. M., Duarte, L. V., & Azerêdo, A. C., 2013. Registo da extinção dos Metacopina
618 (Ostracoda, Crustacea) no Toarciano de Rabaçal, região de Coimbra. Fácies carbonatadas ricas em matéria
619 orgânica do Jurássico da Bacia Lusitânica. Novos contributos paleontológicos, sedimentológicos e
620 geoquímicos. Comunicações Geológicas, 100, 63-68.
621 Capraro, L., Asioli, A., Backman, J., Bertoldi, R., Channell, J. E. T., Massari, F., & Rio, D., 2005. Climatic
622 patterns revealed by pollen and oxygen isotope records across the Matuyama-Brunhes Boundary in the
623 central Mediterranean (southern Italy). Geological Society, London, Special Publications, 247(1), 159-182.
624 Capraro, L., Consolaro, C., Fornaciari, E., Massari, F., Rio, D., 2006. Chronology of the Middle-Upper Pliocene
625 succession in the Strongoli area: constraints on the geological evolution of the Crotone Basin (Southern
626 Italy). In: Moratti, G., Chalouan, A. (Eds.), Tectonics of the Western Mediterranean and North Africa. Geol.
627 Soc. Lond. Spec. Publ. 262 Geological Society, Bath, UK, pp. 323-333.
628 Capraro, L., Massari, F., Rio, D., Fornaciari, E., Backman, J., Channell, J. E. T., Macrì P., Prosser G., Speranza,
629 F., 2011. Chronology of the Lower–Middle Pleistocene succession of the south-western part of the Crotone
630 Basin (Calabria, Southern Italy). Quaternary Science Reviews, 30(9), 1185-1200.

631 Capraro, L., Macrì, P., Scarponi, D., & Rio, D., 2015. The lower to Middle Pleistocene Valle di Manche
632 section (Calabria, Southern Italy): State of the art and current advances. Quaternary International, 383, 36-
633 46.
634 Capraro, L., Ferretti, P., Macrì, P., Scarponi, D., Tateo, F., Fornaciari, E., Bellini G., Dalan, G., 2017. The Valle
635 di Manche section (Calabria, Southern Italy): A high resolution record of the Early-Middle Pleistocene
636 transition (MIS 21-MIS 19) in the Central Mediterranean. Quaternary Science Reviews, 165, 31-48.
637 Ceregato, A., Raffi, S., & Scarponi, D., 2007. The circalittoral/bathyal paleocommunities in the Middle
638 Pliocene of Northern Italy: The case of the *Korobkovia oblonga–Jupiteria concava* paleocommunity
639 type. Geobios, 40(5), 555-572.
640 Cita, M. B., 2008. Summary of Italian marine stages. Episodes, 31(2), 251-254.
641 Cita, M. B., Capraro, L., Ciaranfi, N., Di Stefano, E., Marino, M., Rio, D., Sprovieri R., Vai, G. B., 2006.
642 Calabrian and Ionian: a proposal for the definition of Mediterranean stages for the Lower and Middle
643 Pleistocene. Episodes, 29(2), 107.
644 Colalongo, M. L., & Pasini, G., 1980. La Ostracofauna plio-pleistocenica della Sezione Vrica in Calabria (con
645 considerazioni sul limite Neogene/Quaternario). Bollettino della Società Paleontologica Italiana, 19, 44-126.
646 Cosentino, A., & Giacobbe, S. 2006. A case study of mollusc and polychaete soft-bottom assemblages
647 submitted to sedimentary instability in the Mediterranean Sea. *Marine Ecology*, *27*(2), 170-183.
648 Danise, S., & Holland, S. M., 2017. Faunal response to sea-level and climate change in a short-lived seaway:
649 Jurassic of the Western Interior, USA. Palaeontology, 60(2), 213-232.
650 Dominici, S., 2001. Taphonomy and paleoecology of shallow marine macrofossil assemblages in a collisional
651 setting (late Pliocene–early Pleistocene, western Emilia, Italy). Palaios, 16(4), 336-353.
652 Dominici, S., Conti, C., & Benvenuti, M. 2008. Foraminifer communities and environmental change in
653 marginal marine sequences (Pliocene, Tuscany, Italy). Lethaia, 41(4), 447-460.
654 Fanget, A. S., Bassetti, M. A., Fontanier, C., Tudryn, A., & Berné, S., 2016. Sedimentary archives of climate
655 and sea-level changes during the Holocene in the Rhône prodelta (NW Mediterranean Sea). Climate of the
656 Past, 12(12), 2161.

657 Faranda, C., Gliozzi, E., & Ligios, S., 2007. Late Miocene brackish Loxoconchidae (Crustacea, Ostracoda) from
658 Italy. Geobios, 40(3), 303-324.
659 Faranda, C., & Gliozzi, E., 2008. The ostracod fauna of the Plio-Pleistocene Monte Mario succession (Roma,
660 Italy). Bollettino della Società Paleontologica Italiana, 47(3), 215-267.
661 Frezza, V., & Di Bella, L., 2015. Distribution of recent ostracods near the Ombrone River mouth (Northern
662 Tyrrhenian Sea, Italy). Revue de micropaléontologie, 52(1), 43-66.
663 Gliozzi, E., & Grossi, F., 2008. Late Messinian lago-mare ostracod palaeoecology: A correspondence analysis
664 approach. Palaeogeography, Palaeoclimatology, Palaeoecology, 264(3), 288-295.
665 Gliozzi, E., Pugliese, M., & Alvarez Zarikian, C., 2015. Preface Ostracoda as proxies for paleoenvironmental
666 changes. Palaeogeography Palaeoclimatology Palaeoecology, 419, 1-2.
667 Grossi, F., Gliozzi, E., Anadón, P., Castorina, F., & Voltaggio, M., 2015. Is *Cyprideis agrigentina* Decima a
668 good paleosalinometer for the Messinian Salinity Crisis? Morphometrical and geochemical analyses from
669 the Eraclea Minoa section (Sicily). Palaeogeography, Palaeoclimatology, Palaeoecology, 419, 75-89.
670 Head, M. J., & Gibbard, P. L., 2015. Formal subdivision of the Quaternary System/Period: Past, present, and
671 future. Quaternary International, 383, 4-35.
672 Henderson, P. A., 1990. Freshwater ostracods: keys and notes for the identification of the species. Estuarine
673 and Coastal Sciences Association (Eds.), Linnean Society of London and the Estuarine and Coastal Sciences
674 Association.
675 Horne, D., Holmes, J., Viehberg, F., Rodriguez-Lazaro, J., 2012. Ostracoda as proxies for Quaternary climate
676 change (Vol. 17). Newnes.
677 Horton, B. P., Engelhart, S. E., Hill, D. F., Kemp, A. C., Nikitina, D., Miller, K. G., & Peltier, W. R., 2013.
678 Influence of tidal-range change and sediment compaction on Holocene relative sea-level change in New
679 Jersey, USA. Journal of Quaternary Science, 28(4), 403-411.
680 Huntley, J. W., & Scarponi, D., 2015. Geographic variation of parasitic and predatory traces on mollusks in
681 the northern Adriatic Sea, Italy: implications for the stratigraphic paleobiology of biotic
682 interactions. Paleobiology, 41(1), 134-153.
683 Jackson, D. A., & Somers, K. M., 1991. The spectre of 'spurious' correlations. Oecologia, 86(1), 147-151.

684 Kowalewski, M., Wittmer, J. M., Dexter, T. A., Amorosi, A., & Scarponi, D., 2015. Differential responses of
685 marine communities to natural and anthropogenic changes. Proceedings of the Royal Society of London B:
686 Biological Sciences, 282(1803), 20142990.
687 Laut, L. L. M., Clemente, I. M. M. M., Belart, P., Martins, M. V. A., Frontalini, F., Laut, V. M., Gomes, A.,
688 Boski, T., Lorini, M. L., Fortes, R. R., Rodrigues, M. A. C., 2016. Multiproxies (benthic foraminifera, ostracods
689 and biopolymers) approach applied to identify the environmental partitioning of the Guadiana River
690 Estuary (Iberian Peninsula). Journal of Sedimentary Environments, 1(2), 184-201.
691 Ligios, S., Benvenuti, M., Gliozzi, E., Papini, M., & Rook, L., 2008. Late Miocene palaeoenvironmental
692 evolution of the Baccinello–Cinigiano Basin (Tuscany, central Italy) and new autoecological data on rare
693 fossil fresh-to brackish-water ostracods. Palaeogeography, Palaeoclimatology, Palaeoecology, 264(3), 277-
694 287.
695 Macrì, P., Speranza, F. & Capraro, L., 2014. Magnetic fabric of Plio-Pleistocene sediments from the Crotone
696 fore-arc basin: insights on the recent tectonic evolution of the Calabrian Arc (Italy), J. Geodyn., 81, 67-79.
697 Marco-Barba, J., Mesquita-Joanes, F., & Miracle, M. R., 2013a. Ostracod palaeolimnological analysis reveals
698 drastic historical changes in salinity, eutrophication and biodiversity loss in a coastal Mediterranean
699 lake. The Holocene, 23(4), 556-567.
700 Marco-Barba, J., Holmes, J. A., Mesquita-Joanes, F., & Miracle, M. R., 2013b. The influence of climate and
701 sea-level change on the Holocene evolution of a Mediterranean coastal lagoon: Evidence from ostracod
702 palaeoecology and geochemistry. Geobios, 46(5), 409-421.
703 Marino, M., Bertini, A., Ciaranfi, N., Aiello, G., Barra, D., Gallicchio, S., Girone A., La Perna R., Lirer F.,
704 Maiorano P., Petrosino, P., Toti F., 2015. Paleoenvironmental and climatostratigraphic insights for Marine
705 Isotope Stage 19 (Pleistocene) at the Montalbano Jonico succession, south Italy. Quaternary
706 International, 383, 104-115.
707 Marriner, N., & Morhange, C., 2007. Geoscience of ancient Mediterranean harbours. Earth-Science
708 Reviews, 80(3), 137-194.

709 Martinez-Garcia, B., Rodriguez-Lazaro, J., Pascual, A., & Mendicoa, J., 2015. The “Northern guests” and
710 other palaeoclimatic ostracod proxies in the late Quaternary of the Basque Basin (S Bay of
711 Biscay). Palaeogeography, Palaeoclimatology, Palaeoecology, 419, 100-114.
712 Massari, F., Sgavetti, M., Rio, D., D'alessandro, A., & Prosser, G., 1999. Composite sedimentary record of
713 falling stages of Pleistocene glacio-eustatic cycles in a shelf setting (Crotone basin, south Italy). Sedimentary
714 Geology, 127(1), 85-110.
715 Massari, F., Rio, D., Sgavetti, M., Prosser, G., D'alessandro, A., Asioli, A., ... & Tateo, F., 2002. Interplay
716 between tectonics and glacio-eustasy: Pleistocene succession of the Crotone basin, Calabria (southern
717 Italy). Geological Society of America Bulletin, 114(10), 1183-1209.
718 Massari, F., Capraro, L., & Rio, D., 2007. Climatic modulation of timing of systems-tract development with
719 respect to sea-level changes (middle Pleistocene of Crotone, Calabria, southern Italy). Journal of
720 Sedimentary Research, 77(6), 461-468.
721 Massari, F., Prosser, G., Capraro, L., Fornaciari, E., Consolaro, C., 2010. A revision of the stratigraphy and
722 geology of the south-western part of the Crotone basin (Southern Italy). Ital. J. Geosci. 129, 353-384.
723 Mazzini, I., Anadon, P., Barbieri, M., Castorina, F., Ferreli, L., Gliozzi, E., Mola M., Vittori, E., 1999. Late
724 Quaternary sea-level changes along the Tyrrhenian coast near Orbetello (Tuscany, central Italy):
725 palaeoenvironmental reconstruction using ostracods. Marine Micropaleontology, 37(3), 289-311.
726 Mazzini, I., Goiran, J. P., & Carbonel, P., 2015. Ostracodological studies in archaeological settings: a
727 review. Journal of Archaeological Science, 54, 325-328.

728 Mazzini, I., Rossi, V., Da Prato, S. & Ruscito, V., 2017. Ostracods in archaeological sites along the
729 Mediterranean coastlines: three case studies from the Italian peninsula. In: Williams, M., Hill, T., Boomer, I.
730 & Wilkinson, I. P. (Eds.), The Archaeological and Forensic Applications of Microfossils: A Deeper
731 Understanding of Human History. The Micropalaeontological Society, Special Publications, Geological
732 Society, London, 121–142.

733 McCune, B., Grace, J. B., & Urban, D. L., 2002. Analysis of ecological communities (Vol. 28). Gleneden Beach:
734 MjM software design.

735 Montenegro, M. E., & Pugliese, N., 1996. Autoecological remarks on the ostracod distribution in the
736 Marano and Grado Lagoons (Northern Adriatic Sea, Italy). Bollettino della Società Paleontologica Italiana, 3,
737 123-132.
738 Murray, J. W., 2006. Ecology and applications of benthic foraminifera. Cambridge University Press.
739 Negri, A., Amorosi, A., Antonioli, F., Bertini, A., Florindo, F., Lurcock, P. C., Marabini, S., Mastronuzzi, G.,
740 Regattieri E., Rossi V., Scarponi, D., Taviani M., Zanchetta G., Vai G.B., 2015. A potential global boundary
741 stratotype section and point (GSSP) for the Tarentian Stage, Upper Pleistocene, from the Taranto area
742 (Italy): Results and future perspectives. Quaternary International, 383, 145-157.
743 Pascual, A., Rodriguez-Lazaro, J., Martín-Rubio, M., Jouanneau, J. M., & Weber, O., 2008. A survey of the
744 benthic microfauna (foraminifera, Ostracoda) on the Basque shelf, southern Bay of Biscay. Journal of
745 Marine Systems, 72(1), 35-63.
746 Patzkowsky, M. E., & Holland, S. M., 2012. Stratigraphic paleobiology: understanding the distribution of
747 fossil taxa in time and space. University of Chicago Press.
748 Pint, A., Frenzel, P., Horne, D. J., Franke, J., Daniel, T., Burghardt, A., Wennrich, V., 2015. Ostracoda from
749 inland waterbodies with saline influence in Central Germany: Implications for palaeoenvironmental
750 reconstruction. Palaeogeography, Palaeoclimatology, Palaeoecology, 419, 37-46.
751 Rio, D., Channell, J. E. T., Massari, F., Poli, M. S., Sgavetti, M., D'alessandro, A., & Prosser, G., 1996. Reading
752 Pleistocene eustasy in a tectonically active siliciclastic shelf setting (Crotone peninsula, southern
753 Italy). Geology, 24(8), 743-746.
754 Ritter, M. N., & Erthal, F., 2013. Fidelity bias in mollusk assemblages from coastal lagoons of southern
755 Brazil. Revista Brasileira de Paleontologia, 16(2), 225-236.
756 Roda, C., 1964. Distribuzione e facies dei sedimenti Neogenici nel Bacino Crotonese. Geologica
757 Romana, 3(1964), 319-366.
758 Rossi, S., & Sartori, R., 1981. A seismic reflection study of the external Calabrian Arc in the northern Ionian
759 Sea (eastern Mediterranean). Marine Geophysical Researches, 4(4), 403-426.

760 Rossi, V., Amorosi, A., Sarti, G., & Mariotti, S., 2017. Late Quaternary multiple incised-valley systems: An
761 unusually well-preserved stratigraphic record of two interglacial valley-fill successions from the Arno plain
762 (northern Tuscany, Italy). Sedimentology (in press).
763 Scarponi, D., & Kowalewski, M., 2004. Stratigraphic paleoecology: Bathymetric signatures and sequence
764 overprint of mollusk associations from upper Quaternary sequences of the Po Plain, Italy. Geology, 32(11),
765 989-992.
766 Scarponi, D., & Kowalewski, M., 2007. Sequence stratigraphic anatomy of diversity patterns: Late
767 Quaternary benthic mollusks of the Po Plain, Italy. Palaios, 22(3), 296-305.
768 Scarponi, D., Huntley, J. W., Capraro, L., & Raffi, S., 2014. Stratigraphic paleoecology of the Valle di Manche
769 section (Crotone Basin, Italy): a candidate GSSP of the Middle Pleistocene. Palaeogeography,
770 Palaeoclimatology, Palaeoecology, 402, 30-43.
771 Scarponi, D., Azzarone, M., Kusnerik, K., Amorosi, A., Bohacs, K.M., Drexler, T.M., Kowalewski, M., 2017.
772 Systematic vertical and lateral changes in quality and time resolution of the macrofossil record: Insights
773 from Holocene transgressive deposits, Po coastal plain, Italy, Marine and Petroleum Geology.
774 Sciuto, F., Rosso, A., Sanfilippo, R., & Maniscalco, R., 2015. New faunistic data on the Pleistocene
775 environmental evolution of the south-western edge of the Hyblean Plateau (SE Sicily). Carnets de Geologie-
776 Notebooks on Geology.
777 Sciuto, F., & Rosso, A., 2008. Distribution pattern of deep-water ostracod assemblages from Lower
778 Pleistocene sediments from Furnari, Sicily. Bollettino-Società Paleontologica Italiana, 47(1), 33.
779 Sciuto, F., & Meli, A., 2015. Ostracod association from Pleistocene sediments along the Ionian coast of SE
780 Sicily. Bollettino della Società Paleontologica Italiana, 54(3), 229-241.
781 Speranza F., Macrì P., Rio D., Fornaciari E. & Consolaro C., 2011. Paleomagnetic evidence for a post-1.2 Ma
782 disruption of the Calabria terrane: consequences of slab breakoff on orogenic wedge tectonics, Geol. Soc.
783 Am. Bull., 123, 925-933, doi: 10.1130/B30214.1.
784 Tanaka, G., Matsushima, Y., & Maeda, H., 2012. Holocene ostracods from the borehole core at Oppama
785 Park, Yokosuka City, Kanagawa Prefecture, central Japan: paleoenvironmental analysis and the discovery of
786 a fossil ostracod with three-dimensionally preserved soft parts. Paleontological Research, 16(1), 1-18.

787 Tyler, C. L., & Kowalewski, M., 2014. Utility of marine benthic associations as a multivariate proxy of
788 paleobathymetry: a direct test from recent coastal ecosystems of North Carolina. PloS one, 9(4), e95711.
789 Van Dijk, J.P., 1994. Late Neogene kinematics of intra-arc oblique shear zones: The Petilia-Rizzuto Fault
790 Zone (Calabrian Arc, Central Mediterranean), Tectonics, 13, 1201-1230.
791 Whatley, R. C., & Maybury, C., 1990, in: Chapman and Hall (Eds.), Ostracoda and global events , London, 3-
792 24.
793 Wittmer, J. M., Dexter, T. A., Scarponi, D., Amorosi, A., & Kowalewski, M., 2014. Quantitative bathymetric
794 models for late Quaternary transgressive-regressive cycles of the Po Plain, Italy. The Journal of
795 Geology, 122(6), 649-670.
796 Yasuhara, M., Hunt, G., Cronin, T. M., Hokanishi, N., Kawahata, H., Tsujimoto, A., & Ishitake, M., 2012.
797 Climatic forcing of Quaternary deep-sea benthic communities in the North Pacific Ocean. Paleobiology,
798 38(1), 162-179.
799

800 **CAPTIONS**

801 **Figure 1.** Geological and stratigraphic framework of the VdM section (slightly modified from Scarponi et al.,
802 2014). (A) Location and geological sketch map of the Crotone Basin and the S. Mauro Marchesato (SMM)
803 sub-basin. (B) The SMM cyclothemic succession and correlation to Marine Isotope Stages (after Massari et
804 al., 2002). Biostratigraphic data (biozone) and subdivision in component units (SM1-3) of the SMM
805 Sandstone are also reported. Note the connection between the Matuyama–Brunhes geomagnetic reversal
806 (mid MIS 19) and the Pitagora ash layer. B: Brunhes chron; M: Matuyama chron.

807 **Figure 2.** Stratigraphy of the middle portion of the VdM section, straddling the Early-Middle Pleistocene
808 transition. Lithofacies codes (see text in Sub-section 2.1), T-R cycles (after Scarponi et al., 2014) and $\delta^{18}O$
809 stratigraphy for the benthic foraminifer *Uvigerina peregrina* are showed (after Capraro et al., 2017). The
810 samples selected for ostracod fauna analysis are also highlighted by a thick horizontal bar.

811 **Figure 3.** Plate showing the SEM images of the key/most abundant ostracod species encountered within
812 the VdM section. Scale bar = 100 μm. All lateral external views. Key: RV = right valve; LV = left valve. 1:

Henryhowella sarsii (G.W. Muller, 1894); LV. 2: Close up of *H. sarsii* surface ornamentation (valve showed in 1.). 3: *Cytheropteron monoceros* (Bonaduce, Ciampo & Masoli, 1975); LV. 4: *Cytheropteron ruggierii* (Pucci 1955); LV. 5: *Cytherella vulgatella* (Aiello, Barra, Bonaduce & Russo, 1996); LV. 6: *Pterygocythereis coronata* (Roemer, 1838); RV. 7: *Bairdia conformis* (Terquem, 1878); RV. 8: *Bosquetina tarentina* (Baird, 1850); RV. 9: *Palmoconcha subrugosa* (Ruggieri 1967); RV. 10: *Sagmocythere versicolor* (G.W. Muller, 1894); LV. 11: *Leptocythere multipunctata* (Seguenza 1883); LV. 12: *Semicytherura ruggierii* (Pucci, 1955); RV. 13: *Aurila convexa* (Baird, 1850); RV.

Figure 4. Relative abundances of selected ostracod taxa from the VdM section in respect to the lithofacies and the T-R cycles reported by Scarponi et al. (2014). Samples containing less than 50 valves are highlighted by an asterisk. Species diversity (Fisher index) values are stratigraphically plotted. Two asterisks indicate the sample barren of ostracods. Lithological legend is reported in Figure 2.

Figure 5. Detrended correspondence analysis (DCA) of ostracod species and VdM samples. Key ostracod extant species, for which an ecologic information is available, are reported in bold. DC1 eigenvalue: 0.331; DC2 eigenvalue: 0.183. Samples are shown as colored squares; each color corresponds to specific lithofacies reported in Fig. 4 (orange–D; yellow–C3; dark green–C2; light green–C1; light blue–B and dark blue–A).

Figure 6. Distribution trend of ostracod ecological groups along the VdM section and vertical patterns in DC1 scores/paleobathymetric estimations based on an integrated ostracod-mollusk gradient analysis. VdM $\delta^{18}O$ stratigraphy and lithofacies are also reported (lithological legend is reported in Figure 2). Samples containing less than 50 valves are highlighted by an asterisk, two asterisks indicate the sample barren of ostracods. The sequence stratigraphic interpretation of the multi-proxy paleoenvironmental data is plotted along with the refined identification of the T-R cycles. TST: transgressive system tract; RST: regressive systems tract; TS: transgressive surface and MFZ: maximum flooding zone.

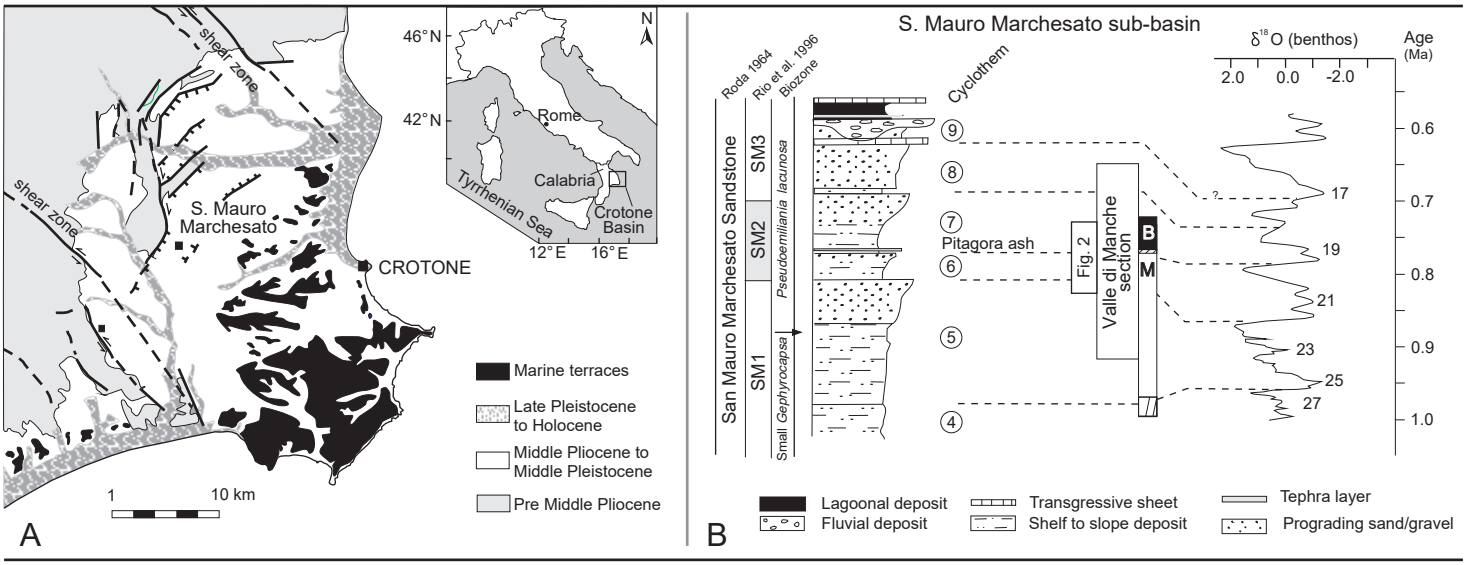

Figure 1 Rossi et al.

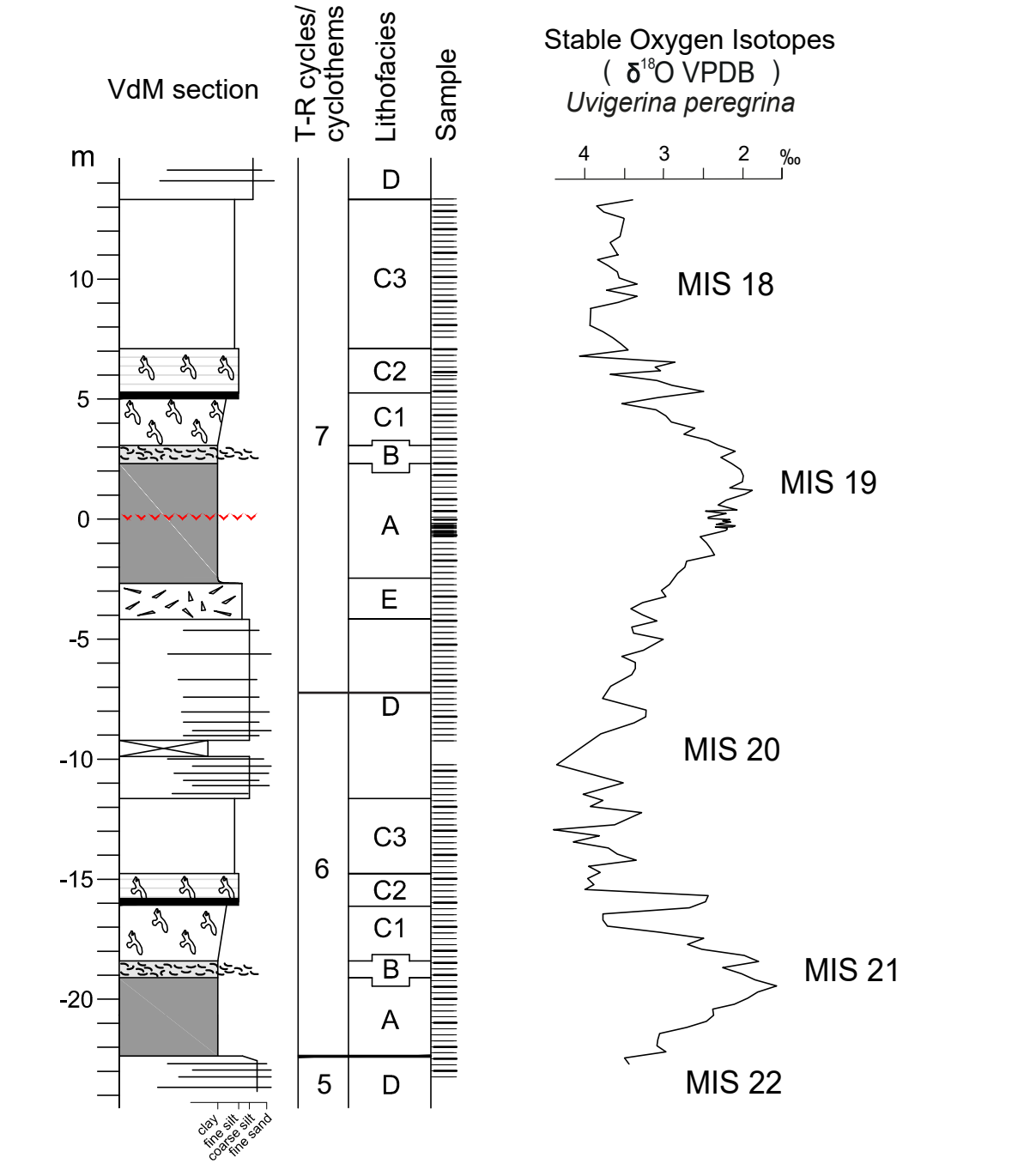

Figure 2 Rossi et al.

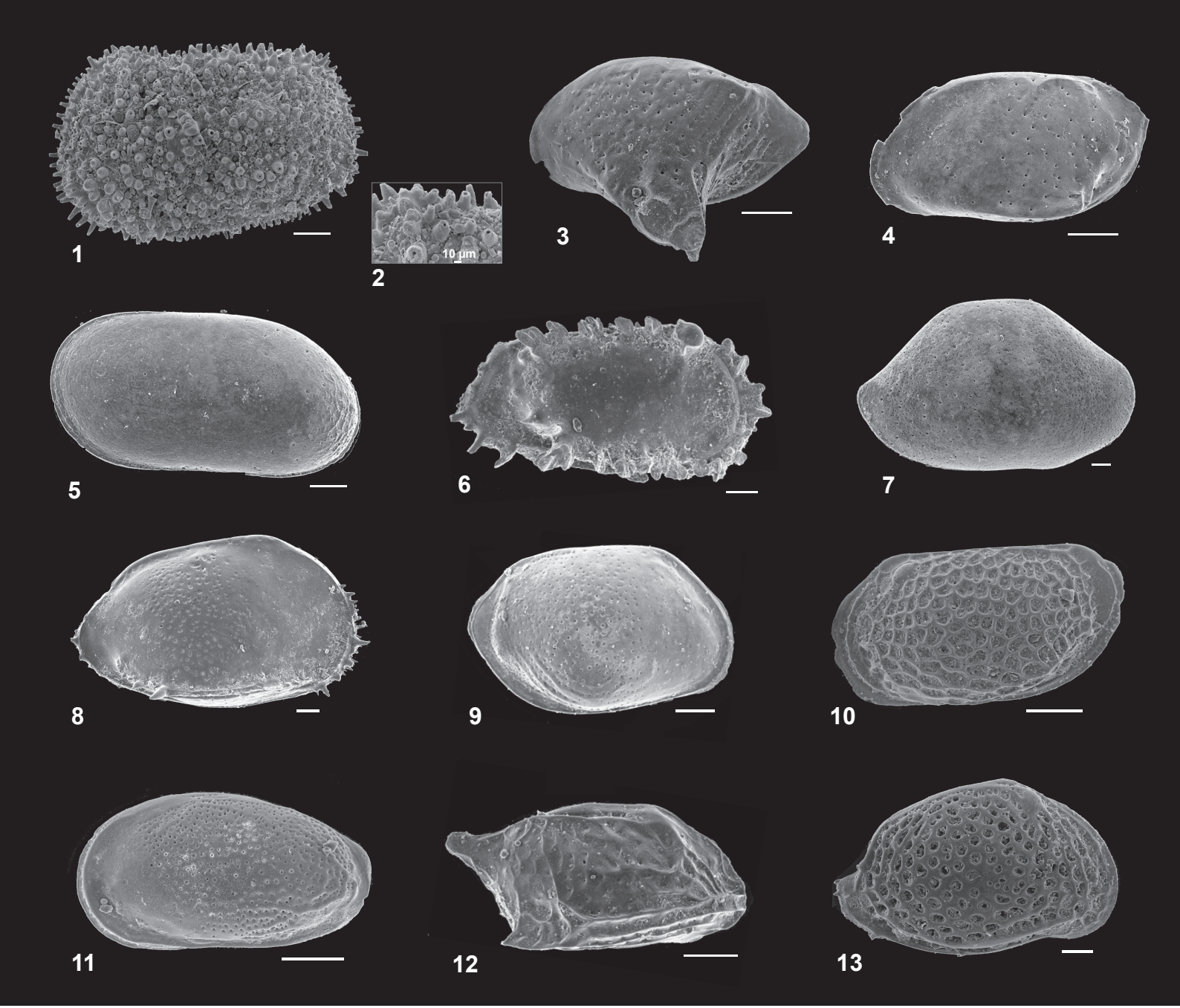

Figure 3 Rossi et al.

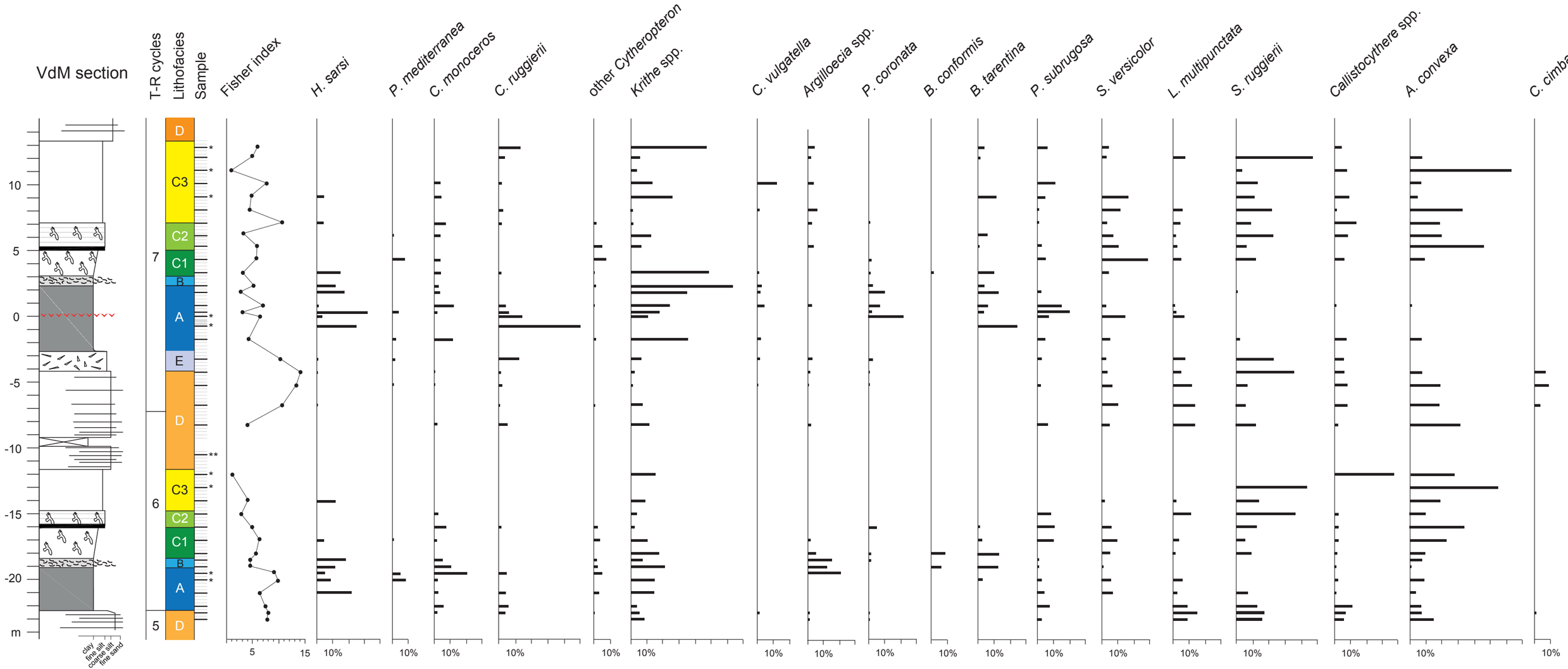

Figure 4 Rossi et al.

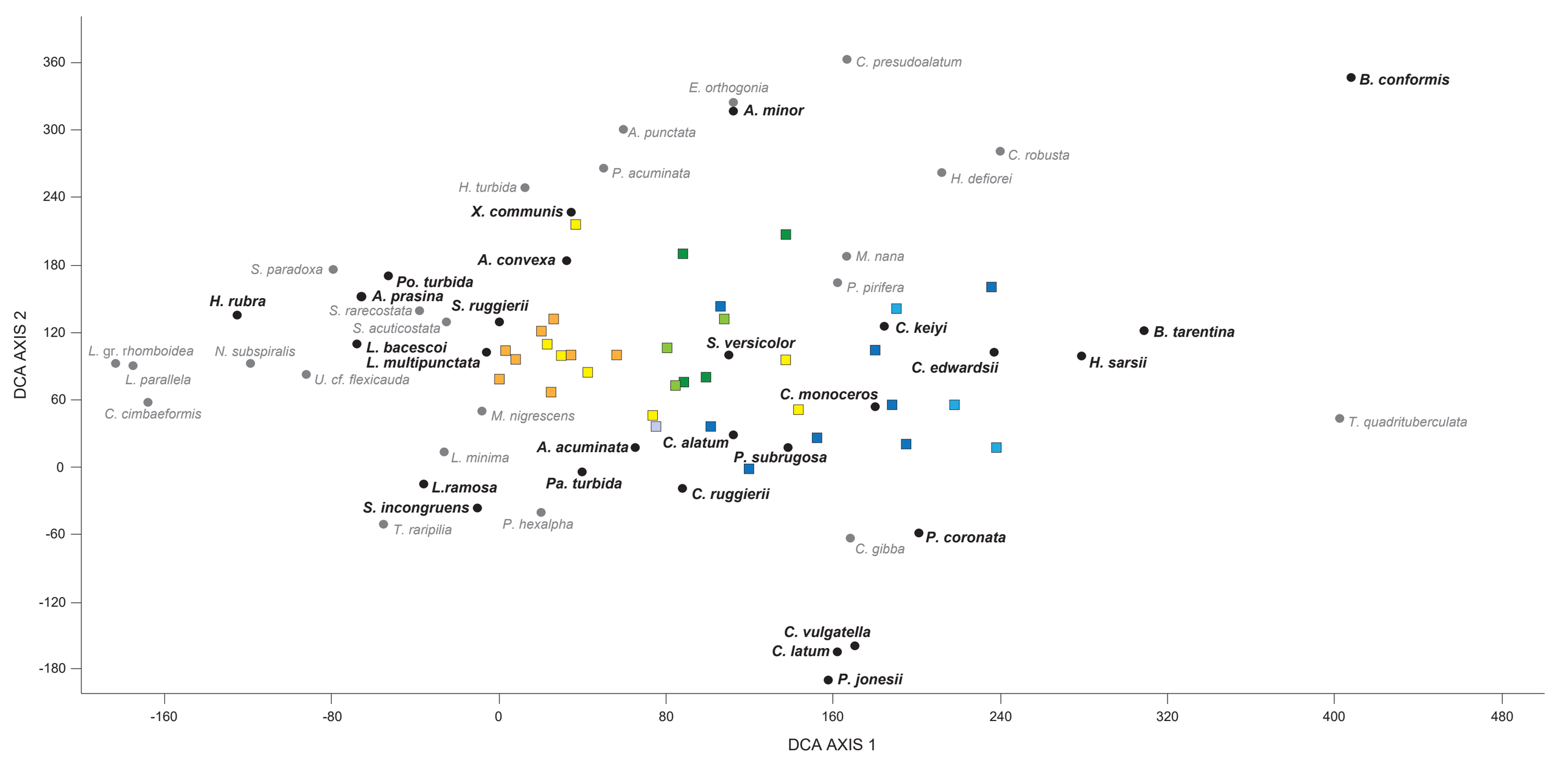

Figure 5 Rossi et al.

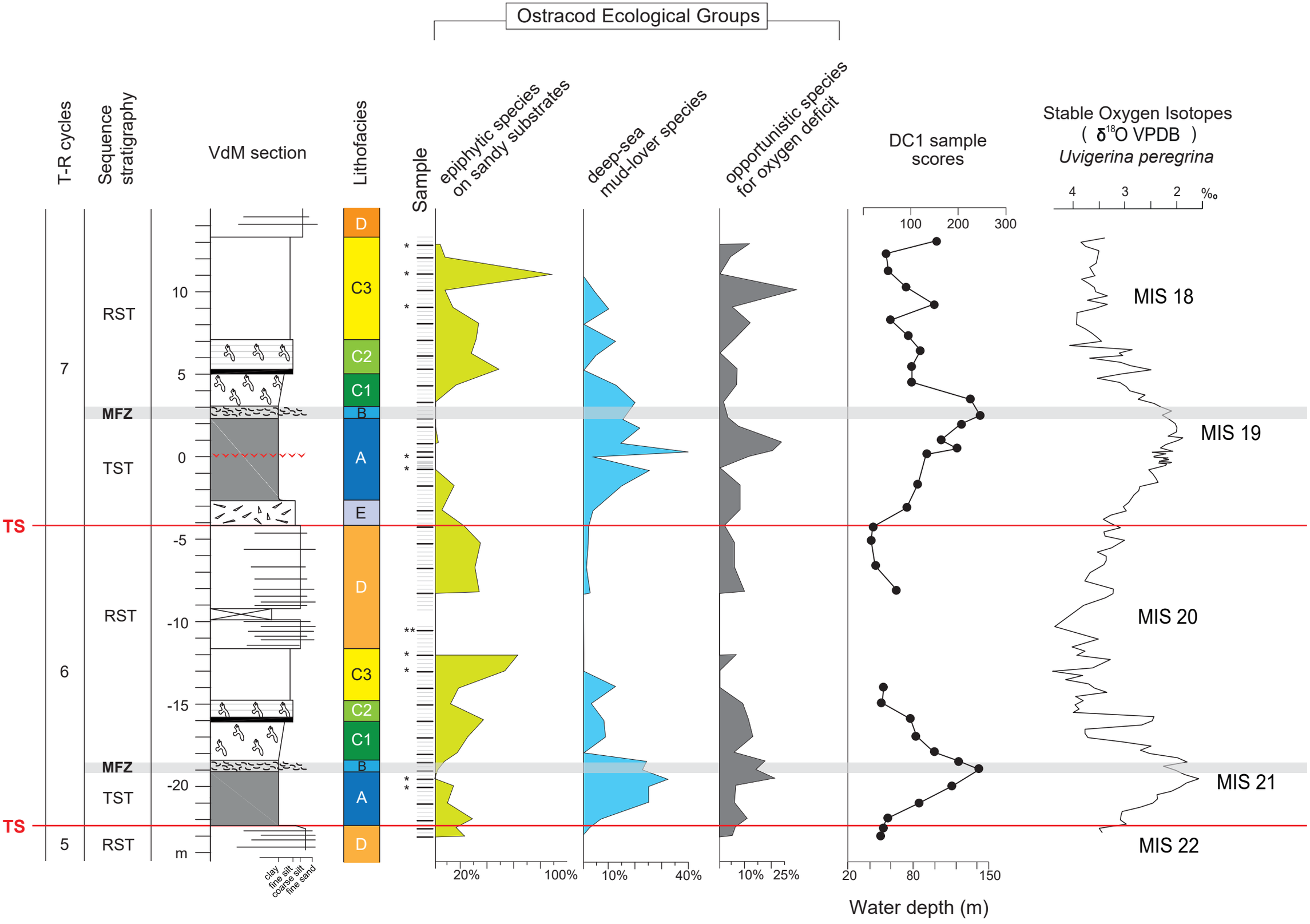

Figure 6 Rossi et al.

SOM Supplementary online material Rossi et al. (submitted) - *Response of ostracod and mollusk marine communities to Early-Middle Pleistocene environmental changes: the Valle di Manche stratigraphic record (GSSP candidate section, Southern Italy*. Palaeogeography, Palaeoclimatology, Palaeoecology

Table S1 - Relevant literature for ostracods taxonomic identification

1	Aiello, G., Barra, D., Abate, S. & Bonaduce, G. 1993: The genus *Parakrithe* van den Bold, 1958 (Ostracoda) in the Pliocene e Early Pleistocene of Sicily. Bollettino della Società Paleontologica Italiana 32 (2), 277–285.
2	Aiello, G., Barra, D., Bonaduce, G. & Russo, A. 1996: The genus *Cytherella* Jones, 1849 (Ostracoda) in the Italian Tortonian e recent. Revue de Micropaleontologie 39 (3), 171–190.
3	Aiello, G., Barra, D. & Bonaduce, G. 2000: Systematic and biostratigraphy of the ostracoda of the Plio-Pleistocene Monte S. Nicola Section (Gela; Sicily). Bollettino della Società Paleontologica Italiana 39 (1), 83–112.
4	Athersuch, J., Horne, D. J. & Whittaker, J. E. 1989: Marine and brackish water ostracods. In Kermack, D. M. & Barnes, R. S. K. (Eds.): Synopses of the British Fauna (New Series) 43, 1–345. Brill E.J., Leiden.
5	Barra, D., Aiello, G. & Bonaduce, G. 1996: The genus *Argilloecia* Sars, 1866 (Crustacea: Ostracoda) in the Pliocene - Early Pleistocene of the M. San Nicola Section (Gela, Sicily). Proceedings of the 2nd European Ostracodologists Meeting, British Micropalaeontological Society, 129–134.
6	Bonaduce, G., Ciampo, G. & Masoli, M. 1975: Distribution of Ostracoda in the Adriatic Sea. Pubblicazione Stazione Zoologica di Napoli 40, 1–304.
7	Breman, E. 1975: The distribution of Ostracodes in the bottom sediments of the Adriatic Sea. Ph.D Thesis, Free University of Amsterdam, 165 pp.
8	Colalongo, M.L. & Pasii, G. 1980: L'ostracofauna plio-pleistocenica della sezione di Vrica in Calabria (con considerazioni sul limite Neogene/Quaternario). Bollettino della Società Paleontologica Italiana 19 (1), 44–126.
9	Faranda, C. & Gliozzi, E. 2008: The ostracod fauna of the Plio-Pleistocene Monte Mario succession (Roma, Italy). Bollettino della Società Paleontologica Italiana 47 (3), 215–267.

Table S2 A - Sample information and major axis sample scores obtained from nonmetric Multi-Dimensional Scaling and Detrended Correspondence Analyses (nMDS and DCA respectively), concerning ostracod and mollusk datasets sampled at Val di Manche. **A1**) Mollusk sample label; **A2**) DCA axis 1 sample score; **A3**) Estimated sample water depth; **A4**) Stratigraphic offset respect to nearest ostracod sample; **A5**) Ostracod sample label; **A6-7**) nMDS axis 1 sample scores obtained from a reduced ostracod matrix (employing absolute—Abs and relative—Rel abundances) comparable in sample size and sampling resolution to the mollusk one (i.e., 17 samples). Stress values = 0.19 and 0.16 respectively. **A8-9**) As for A6-7 but employing DCA. **A10-11**) nMDS axis 1 sample scores obtained from the full ostracod matrix (i.e., 51 taxa and 34 samples) employing absolute—Abs and relative—Rel abundances. Stress values = 0.20 and 0.19 respectively; **A10-11**) As for A6-7 but employing DCA**. B.** Linear correlation (RMA) coefficients (r—Pearson) and p-values (α = 0.05) between ordination major axis of variation (i.e., DCA-1 or nMDS-1) of Ostracod and Mollusc DCA axis 1 sample score (after Scarponi et al., 2014). Correlation analyses varying sample and species structure (reduced or full matrix, relative or raw abundance) all returned high and significant correlation coefficients. Ordination analyses performed with PAST 3.11.

A) Ordination analyses and sample information of Val di Manche Section

Mollusk samples				**Ostracod samples**								
after Scarponi et al. (2014)					**Matrix 17 samples**				**Matrix 34 samples**			
Label	**DCA-1**	**W-depth (m)**	**S-offset (cm)**	**Label**	**nMDS-1**		**DCA-1**		**nMDS-1**		**DCA-1**	
					Abs	**Rel**	**Abs**	**Rel**	**Abs**	**Rel**	**Abs**	**Rel**
1)	**2)**	**3)**	**4)**	**5)**	**6)**	**7)**	**8)**	**9)**	**10)**	**11)**	**12)**	**13)**
Bk22	196	-55	20	SMA50	-0.24433	-0.25854	22	0	0.121	0.128	15	31
Bk21	117	-84	0	SMA42	-0.05252	-0.04989	87	73	0.012	0.014	94	74
Bk20	95	-92	-40	SMA38	0.14789	0.084843	143	127	-0.067	-0.047	135	137
Bk19	122	-82	0	SMA30	-0.10886	-0.10742	67	57	0.051	0.052	79	80
Bk18	67	-103	-10	SMA18	-0.03471	-0.02284	109	61	0.043	0.042	83	88
Bk17	0	-128	40	SMA10	0.41237	0.41683	264	237	-0.307	-0.282	255	238
Bk16	9	-124	-30	SMA8	0.31321	0.33418	206	218	-0.245	-0.237	235	195
Bk15	51	-109	0	SMA4	0.16096	0.18789	173	151	-0.133	-0.160	174	152
Bk14	90	-94	40	SMA-8	0.073954	0.078073	142	106	-0.051	-0.072	118	102
Bk13	98	-91	-20	SMA-14	-0.16361	-0.16797	91	41	0.055	0.048	80	76
Bk12	223	-45	10	SMB14	-0.18192	-0.21069	29	11	0.145	0.145	20	8
Bk11	198	-54	10	SMB20	-0.14185	-0.15454	56	14	0.090	0.095	38	56
Bk9	164	-67	30	SMB40	-0.24981	-0.20625	0	30	0.117	0.096	45	26
Bk8	80	-98	20	SMB52	-0.04612	-0.05474	96	70	0.026	0.019	91	99
Bk7	59	-106	10	SMB56	-0.02318	0.030985	84	157	0.037	0.025	134	137
Bk6	4	-126	0	SMB60	0.35609	0.32507	181	257	-0.224	-0.229	267	236
Bk5	272	-26	60	SMB76	-0.21757	-0.22499	2	5	0.136	0.136	24	20

B) Residual Major Axis linear correlation

Ostracod 17 samples matrix *vs.* DCA-1 Mollusk dataset		**Ostracod 34 samples matrix *vs.* DCA-1 Mollusk dataset**	
n-MDS-1 absolute abundance	r = -0.844, p << 0.05	*n-MDS-1 absolute abundance*	r = 0.849, p << 0.05
n-MDS-1 relative abundance	r = -0.873, p << 0.05	*n-MDS-1 relative abundance*	r = 0.864, p << 0.05
DCA-1 log-transformed raw values	r = -0.881, p << 0.05	*DCA-1 log-transformed raw value*	r = 0.894, p << 0.05
DCA-1 relative abundance	r = -0.880, p << 0.05	*DCA-1 relative abundance*	r = -0.905, p << 0.05

Table S3 A - Age, grain size information and DCA sample scores obtained from full ostracod matrix (i.e., 51 species and 34 samples, log transformed absolute values) at Val di Manche. DCA performed with PAST 3.11. Age model was obtained by tuning the *Uvigerina peregrina* oxygen isotope record to the Mediterranean stack by Wang et al. (2010) (see Capraro et al, 2017 for further details). **B**. Linear correlation coefficient (r—Pearson) and p-values (α = 0.05) between DCA 1 sample scores and % of sand in each sample are shown.

A)	**Ostracod dataset: sample age, grain size and DCA score**					
Label	Position (m)	Age (ky)	Sample_weight (gr)	Grain size fraction >63 micron (gr)	sandy fraction	DCA1 sample score
SMA53	12.81	741.8	46.9	2.7	5.7	164
SMA50	12.06	744.4	48.0	6.1	12.8	15
SMA46	11.06	747.8	50.8	1.4	2.8	4
SMA42	10.06	751.2	46.9	8.6	18.3	94
SMA38	9.06	754.6	48.8	3.3	6.7	135
SMA34	8.06	758.0	47.4	9.0	19.0	34
SMA30	7.06	761.2	45.4	14.4	31.7	79
SMA26	6.21	764.0	47.7	5.1	10.8	55
SMA22	5.31	767.0	54.9	1.5	2.7	41
SMA18	4.31	770.1	55.0	3.3	6.1	83
SMA14	3.31	773.4	57.2	3.2	5.6	242
SMA10	2.31	777.5	55.3	3.4	6.2	255
SMA8	1.81	780.0	56.2	5.1	9.1	235
SMA4	0.81	784.5	55.0	1. 9	3.4	174
SMA2	0.31	786.3	58.5	1.5	2.6	238
SMA-1	0.00	787.5	51.8	2.6	5.0	151
SMA-8	-1.75	794.0	46.6	3.9	8.4	118
SMA-14	-3.25	795.6	46.4	6.8	14.6	80
SMB4	-4.25	796.7	54.9	11.4	20.8	0
SMB8	-5.25	797.7	57.1	7.8	13.7	2
SMB14	-6.75	799.3	56.2	3.5	6.3	20
SMB20	-8.25	800.9	55.1	4.8	8.7	38
SMB40	-14.00	811.6	54.0	5.0	9.2	45
SMB44	-15.00	813.8	50.1	19.8	39.4	20
SMB48	-16.00	827.3	54.5	21.3	39.1	66
SMB52	-17.00	839.4	55.5	6.0	10.9	91
SMB56	-18.00	846.3	55.0	18.2	33.1	134
SMB58	-18.50	850.6	53.8	6.1	11.4	240
SMB60	-19.00	855.8	56.4	6.8	12.0	267
SMB64	-20.00	861.9	53.5	1.3	2.4	204
SMB68	-21.00	863.6	54.9	6.8	12.4	162
SMB72	-22.00	865.3	54.9	4.6	8.3	52
SMB74	-22.50	866.1	50.4	4.0	8.0	25
SMB76	-23.00	867.0	54.6	8.5	15.6	24

B)	**Residual Major Axis linear correlation**		
	DCA score *vs.* % of sand		
r= -0.291	r2 = 0.085	p = 0.094	

Table S4 - Bathymetric calibration of ostracod samples. Bathymetric estimates are derived by linear correlation between a subset of DCA axis one ostracod sample scores (i.e.. Table 2A column 12) and previously derived water depth estimates of mollusk samples previously collected (i.e.. Table 2A column 3). within the same stratigraphic interval (see Table S2A column 4). Residual major axis regression coefficients: slope a = -0.36615; intercept b = -46.651; r = -0.89; p < 0.0001; standard error of the estimates = 13.3 m.

Ostracod dataset: bathymetric sample estimates			
Label	**Strat_position (m)**	**DCA 1 sample core**	**W-depth**
SMA53	12.81	164	-107
SMA50	12.06	15	-52
SMA46	11.06	4	-48
SMA42	10.06	94	-81
SMA38	9.06	135	-96
SMA34	8.06	34	-59
SMA30	7.06	79	-76
SMA26	6.21	55	-67
SMA22	5.31	41	-62
SMA18	4.31	83	-77
SMA14	3.31	242	-135
SMA10	2.31	255	-140
SMA8	1.81	235	-133
SMA4	0.81	174	-110
SMA2	0.31	238	-134
SMA-1	0	151	-102
SMA-8	-1.75	118	-90
SMA-14	-3.25	80	-76
SMB4	-4.25	0	-47
SMB8	-5.25	2	-47
SMB14	-6.75	20	-54
SMB20	-8.25	38	-61
SMB40	-14	45	-63
SMB44	-15	20	-54
SMB48	-16	66	-71
SMB52	-17	91	-80
SMB56	-18	134	-96
SMB58	-18.5	240	-135
SMB60	-19	267	-144
SMB64	-20	204	-121
SMB68	-21	162	-106
SMB72	-22	52	-66
SMB74	-22.5	25	-56
SMB76	-23	24	-55

Figure S1 - nMDS ordination outputs using Bray-Curtis pairwise comparison and employing (**A**) absolute and (**B**) relative abundance data. The data matrix includes only samples with more than 20 specimens (34 samples) and species recorded in more than one sample (51 species; Appendix 1). nMDS analyses performed in R (version 3.3.2)

Figure S2 – non-Metric Multidimensional Scaling (nMDS) axis 1 sample scores plotted stratigraphically along VdM section. Both ordinations returned comparable patterns. Results obtained employing absolute (**A**) and relative (**B**) abundance data-matrix (see also Fig. S1). Analyses performed in R (version 3.3.2)

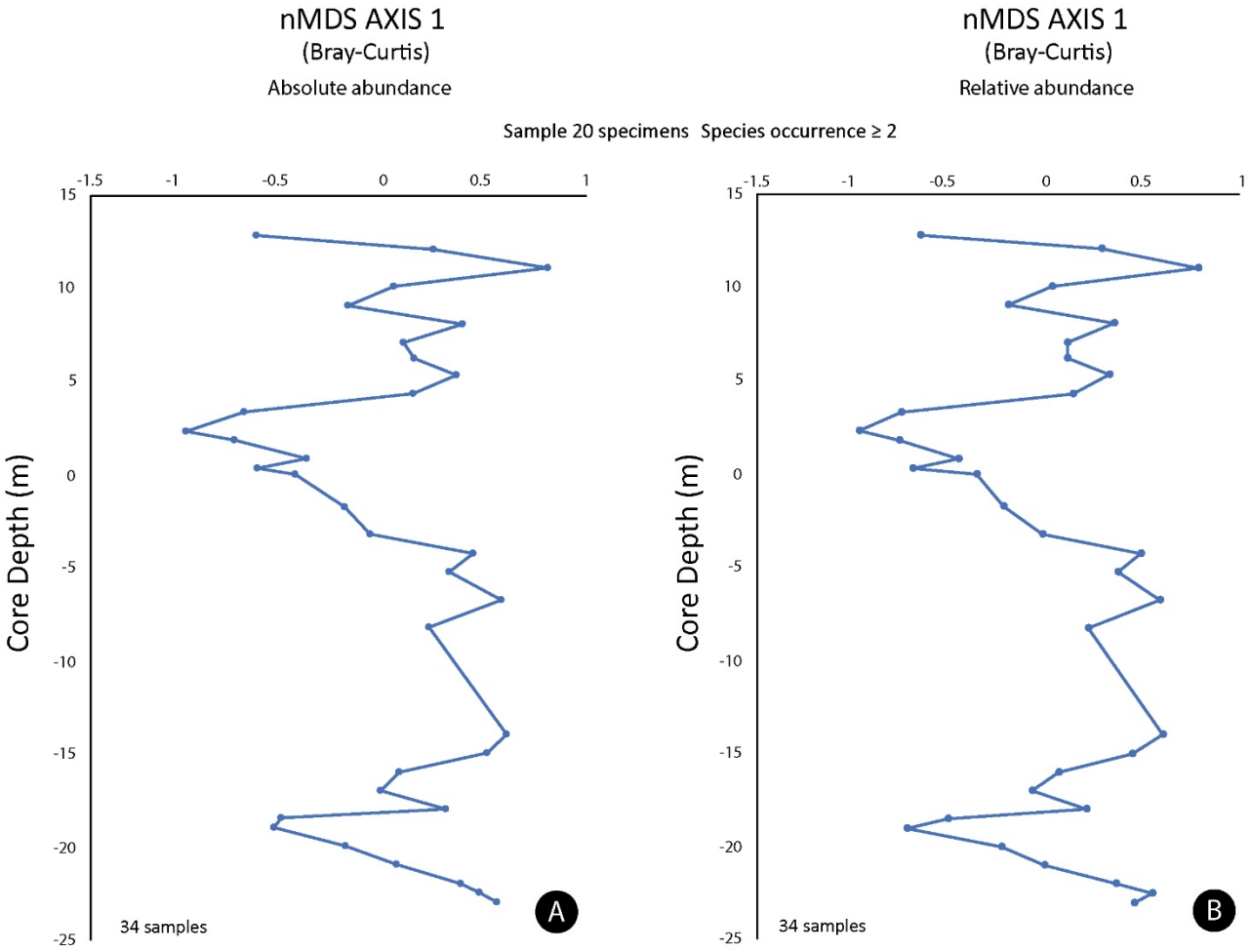

Figure S3 – Detrended Correspondence Analysis (**A**. **C**. **E**) and non-metric Multidimensional Scaling (**B**. **D**. **F**) on log-transformed. absolute abundance data-matrix; varying taxa or sample thresholds returned comparable patterns. Here reported sample axis 1 scores plotted stratigraphically. **A-B**) sample size ≥ 20 specimens and species singletons excluded. **C-D**) sample size ≥ 25 specimens and species occurrences ≥ 5 samples. **E-F**) reduced ostracod dataset (17 samples/34 species) comparable (in sample size and sampling resolution) to the mollusk dataset reported in Scarponi et al.. 2014; sample size ≥ 20 specimens and species singletons excluded. Analyses performed in R (version 3.3.2).

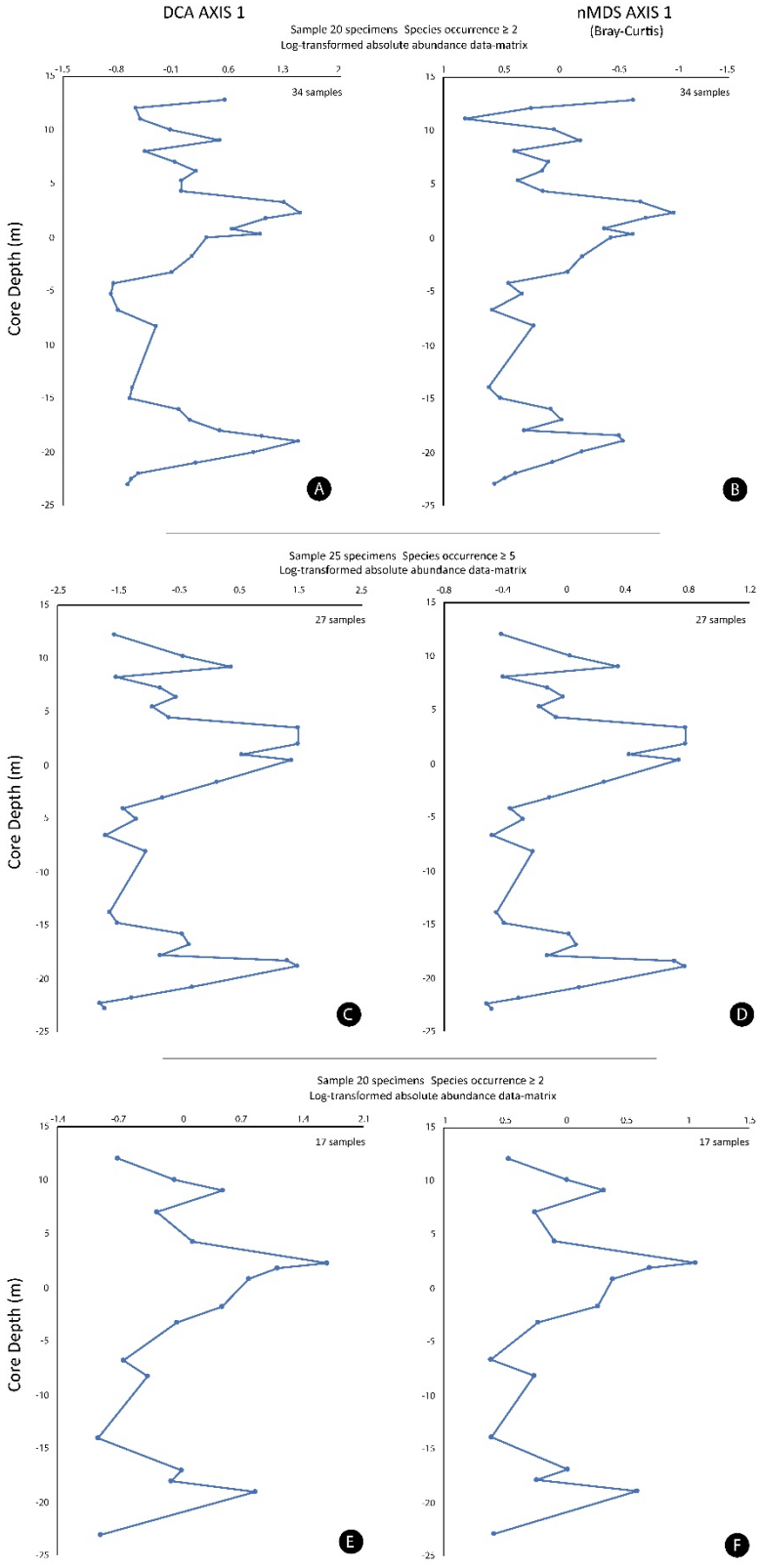

References

Capraro. L.. Ferretti. P.. Macrì. P.. Scarponi. D.. Tateo. F.. Fornaciari. E.. Bellini G.. Dalan. G.. 2017. The Valle di Manche section (Calabria. Southern Italy): A high resolution record of the Early-Middle Pleistocene transition (MIS 21-MIS 19) in the Central Mediterranean. Quaternary Science Reviews. 165. 31-48.

Scarponi. D.. Huntley. J. W.. Capraro. L.. & Raffi. S. 2014. Stratigraphic paleoecology of the Valle di Manche section (Crotone Basin. Italy): a candidate GSSP of the Middle Pleistocene. Palaeogeography. Palaeoclimatology. Palaeoecology. 402. 30-43.

Wang. P.. Tian. J.. Lourens. L.J.. 2010. Obscuring of long eccentricity cyclicity in Pleistocene oceanic carbon isotope records. Earth and Planetary Science Letters. 290(3-4). 319-330. doi:10.1016/j.epsl.2009.12.02

SOM-Appendix 1. Ostracod Dataset with specimens counts for each sample. Symbol "*"= taxa and samples removed to generate 51 species and 34 sample matrix; "**" = removed to generate 40 species and 17 samples matrix.

Ostracod taxon/Sample position (m)	**		**			**		**	**
	SMA53	SMA50	SMA46	SMA42	SMA38	SMA34	SMA30	SMA26	SMA22
	12.81	12.06	11.06	10.06	9.06	8.06	7.06	6.21	5.31
Aurila convexa (Baird, 1850)	0	8	16	7	2	43	33	19	35
Cimbaurila cimbaeformis (Seguenza, 1883) **	0	0	0	0	0	0	0	0	0
Aurila cruciata (Ruggieri, 1950) */**	0	0	0	0	0	0	0	0	0
Aurila interpretis (Uliczny, 1969) */**	0	0	0	0	0	0	0	0	0
Aurila prasina (Barbeito-Gonzalez, 1971)	0	0	0	1	0	0	0	0	0
Aurila punctata (Münster, 1830) **	0	0	5	0	0	0	0	0	3
Aurila sp. */**	0	0	0	0	0	0	0	0	0
Callistocythere group (Ruggieri, 1953) */**	2	0	2	0	4	2	24	8	0
Carinocythereis carinata (Roemer, 1838) */**	0	0	0	0	0	0	0	0	0
Cluthia keiyi (Neale, 1975)	0	0	0	0	0	0	3	2	1
Costa edwardsii (Roemer, 1838) **	1	0	0	0	0	0	0	0	0
Cytherois sp. */**	0	0	0	0	0	0	0	0	0
Cytheromorpha nana (Bonaduce, Ciampo & Masoli, 1975) */**	0	0	0	0	0	0	0	0	0
Cytheromorpha fuscata (Brady, 1869) */**	0	0	0	0	0	0	0	0	0
Eucythere curta (Ruggieri, 1975) */**	0	0	0	0	0	0	0	0	0
Eucythere pubera (Bonaduce, Ciampo & Masoli, 1975) */**	0	0	0	0	0	0	0	0	0
Eucytherura orthogonia (Colalongo & Pasini, 1980)	0	0	0	0	0	0	2	5	2
Hiltermannicythere rubra (G.W. Muller, 1894)	0	2	0	0	0	0	1	0	0
Hiltermannicythere turbida (G.W. Muller, 1894) **	0	0	0	0	0	0	0	0	0
Loxoconcha geometrica (Bonaduce, Ciampo & Masoli, 1975) */**	0	0	0	1	0	0	0	0	0
Loxoconcha minima(Bonaduce et al., 1975) **	1	0	0	0	0	0	0	0	0
Loxoconcha parallela (G.W. Muller, 1894) **	0	0	0	0	0	0	0	0	0
Loxoconcha gr. rhomboidea (Fischer, 1855) **	0	0	0	0	0	0	0	0	0
Loxoconcha sp. */**	0	0	0	0	0	0	0	0	0
Macrocypris sp. */**	0	0	0	0	0	0	2	0	0
Neocytherideis subspiralis (Brady, Crosskey & Robertson, 1874) **	0	0	0	0	0	1	0	0	0
Neocytherideis sp. */**	0	0	0	0	0	0	0	0	0
Occultocythereis sp. */**	0	0	0	1	0	0	0	0	0
Paracytheridea hexalpha (Doruk, 1980)	0	0	0	0	0	2	2	0	0
Paracytheridea sp. */**	0	0	0	0	0	0	0	0	0
Pontocypris acuminata (G.W. Muller, 1894)	0	0	0	0	0	0	0	0	0
Pontocythere turbida (G.W. Muller, 1894)	0	0	0	0	0	1	2	0	0
Propontocypris pirifera (G.W. Muller, 1894) **	0	0	0	0	0	1	0	0	0
Sagmocythere versicolor (G.W. Muller, 1894)	2	3	0	0	7	15	6	7	8
Semicytherura acuticostata (G.O. Sars, 1866)	0	0	0	0	0	0	0	0	0
Semicytherura incongruens (G.W. Muller, 1894) **	0	0	0	0	1	0	0	0	0
Semicytherura marialuisae (Faranda & Gliozzi, 2008) */**	0	0	0	0	0	0	0	0	0
Semicytherura paradoxa (G.W. Muller, 1894)	0	4	0	0	0	0	2	0	0
Semicytherura rarecostata (Bonaduce, Ciampo & Masoli, 1975)	0	1	0	0	0	4	4	0	0
Semicytherura ruggierii (Pucci, 1955)	0	48	1	13	5	29	17	22	5
Semicytherura sulcata (G.W. Muller, 1894) */**	0	0	0	0	0	0	0	0	0
Semicytherura sp. */**	0	0	0	0	0	0	0	0	0
Hemicytherura diaforei (Ruggeri, 1953)	2	0	0	0	0	0	3	0	0
Microcytherura angulosa (Seguenza, 1880) */**	0	0	0	0	0	0	0	0	0
Microcytherura nigrescens (G.W. Muller, 1894)	0	0	0	0	0	0	0	0	1
Microcytherura sp. */**	0	0	0	0	0	0	0	0	0
Monoceratina mediterranea (Sissingh, 1972) */**	0	0	0	0	0	0	0	0	0

Tuberculocythere quadrituberculata (Colalongo & Pasini, 1980)	0	0	0	0	0	0	0	0	0
Microxestoleberis nana (G.W. Muller, 1894)	0	0	0	0	0	0	4	0	0
Microxestoleberis xenomys (Barbeito-Gongalez, 1971) */**	0	0	0	2	0	0	0	0	0
Urocythereis cf. *U. flexicauda* (Bonaduce, Ciampo & Masoli, 1975)	0	2	0	2	0	0	0	0	0
Xestoloberis communis (G.W. Muller, 1894)	0	0	0	0	0	2	2	0	1
Xestoloberis sp. */**	0	0	0	0	0	0	0	0	0
Palmoconcha turbida (G.W. Muller, 1894)	0	2	0	1	0	3	3	0	0
Palmoconcha subrugosa (Ruggieri 1967)	3	0	0	11	2	2	2	0	2
Pterygocythereis coronata (Roemer, 1838)	0	0	0	0	0	0	2	0	0
Pterygocythereis jonesii (Baird 1850)	0	0	0	0	0	0	0	0	0
Pterygocythereis sp. */**	0	0	0	0	0	0	0	0	0
Leptocythere bacescoi (Rome 1942)	0	2	0	2	0	0	2	0	0
Leptocythere levis (G.W. Muller, 1894) */**	0	0	0	0	0	0	0	0	0
Leptocythere macella (Ruggieri, 1975) */**	0	0	0	0	0	0	0	0	0
Leptocythere multipunctata (Seguenza 1883)	0	8	0	0	0	8	8	2	2
Leptocythere ramosa (Rome 1942)	0	0	0	1	0	0	1	0	0
Leptocythere rara (G.W. Muller, 1894) */**	0	0	0	0	0	0	0	0	0
Leptocythere transiens (Pucci, 1956) */**	0	0	0	0	0	0	0	0	0
Leptocythere sp. */**	0	0	0	0	0	0	0	0	0
Cytherella alverium (Bonaduce, Ciampo & Masoli, 1975) */**	0	0	0	2	0	0	0	0	0
Cytherella gibba (Aiello, Barra, Bonaduce & Russo, 1996)	2	5	0	7	0	0	3	2	0
*Cytherella robusta (*Colalongo & Pasini, 1980)	0	0	0	0	0	0	0	0	1
Cytherella vulgatella (Aiello, Barra, Bonaduce & Russo, 1996)	0	0	0	12	0	2	0	0	0
Cytherella sp. */**	0	0	0	0	0	0	0	0	0
Argilloecia acuminata (G.W. Muller, 1894)	2	1	0	2	0	8	5	0	0
Argilloecia minor (G.W. Muller, 1894)	0	1	0	2	0	0	0	0	2
Argilloecia robusta (Bonaduce, Ciampo & Masoli, 1975) */**	0	0	0	0	0	0	0	0	0
Argilloecia sp. */**	0	0	0	0	0	0	0	0	1
Bairda conformis (Terquem, 1878)	0	0	0	0	0	0	0	0	0
Bairda sp. */**	0	0	0	0	0	0	0	0	0
Bosquetina tarentina (Baird, 1850)	2	2	0	0	5	0	0	6	1
Bosquetina sp. */**	0	0	0	0	1	0	0	0	0
Cytheropteron aduncum (Colalongo & Pasini, 1980) */**	0	0	0	0	0	0	0	0	0
Cytheropteron agile (Colalongo & Pasini, 1980) */**	0	0	0	0	0	0	0	0	0
Cytheropteron alatum (Sars, 1866)	0	0	0	0	0	0	1	0	0
Cytheropteron cf. C. ionicum (Colalongo & Pasini, 1980) */**	0	0	0	0	0	0	0	0	0
Cytheropteron latum (G.W. Muller, 1894)	0	0	0	0	0	0	0	0	0
Cytheropteron monoceros (Bonaduce, Ciampo & Masoli, 1975)	0	0	0	4	2	0	13	4	0
Cytheropteron pseudoalatum (Colalongo & Pasini, 1980) **	0	0	0	0	0	0	1	0	4
Cytheropteron rectum (Colalongo & Pasini, 1980) */**	0	0	0	0	0	0	0	0	0
Cytheropteron ruggierii (Pucci 1955)	6	4	0	2	0	4	4	0	0
Cytheropteron trapezium (Colalongo & Pasini, 1980) */**	0	0	0	0	0	0	0	0	0
Cytheropteron sp. */**	0	0	0	0	0	0	1	0	0
Henryhowella sarsii (G.W. Muller, 1894)	0	0	0	0	2	0	8	0	0
Krithe group (Brady, Crosskey & Robertson, 1874) */**	21	6	1	13	11	2	3	12	5
Parakrithe group (van den Bold, 1958) */**	0	1	0	9	0	0	9	4	1
Paracytheroismediterranea (Bonaduce, Ciampo & Masoli, 1975)	0	0	0	0	0	0	0	1	0
Triebielina raripilia (G.W. Muller, 1894)	0	0	0	0	0	0	0	0	0
Total Abundance	**44**	**100**	**25**	**95**	**42**	**129**	**173**	**94**	**75**

	**				**	**	*/**				**	**	**		*/**
SMA18	SMA14	SMA10	SMA8	SMA4	SMA2	SMA-1	SMA-4	SMA-8	SMA-14	SMB4	SMB8	SMB14	SMB20	SMB26
4.31	3.31	2.31	1.81	0.81	0.31	0.00	-0.75	-1.75	-3.25	-4.25	-5.25	-6.75	-8.25	-10.5
9	0	0	0	2	0	0	0	9	0	9	24	20	27	0
0	0	0	0	0	0	0	0	0	0	8	11	4	0	0
0	0	0	0	0	0	0	0	0	0	1	0	0	0	0
0	0	0	0	0	0	0	0	0	0	0	0	1	0	0
0	0	0	0	0	0	0	0	0	0	0	0	0	0	0
0	0	0	0	0	0	0	0	0	0	1	0	0	0	0
1	0	0	0	0	0	0	0	0	0	0	0	0	1	0
6	0	0	0	2	0	0	0	9	6	7	10	9	2	0
0	0	0	0	0	0	0	0	0	0	0	1	0	0	0
4	0	2	0	3	0	0	0	0	2	0	0	0	0	0
0	0	0	1	0	0	0	0	0	0	0	0	0	0	0
0	0	0	0	0	0	0	0	0	0	1	0	0	0	0
0	0	0	0	0	0	0	0	0	0	0	1	0	0	0
0	0	0	0	0	0	0	0	0	0	0	0	0	0	0
0	0	0	0	0	0	0	0	0	1	0	0	0	0	0
0	0	0	0	0	0	0	0	0	0	0	0	0	0	0
0	0	0	0	0	0	0	0	0	0	1	6	3	0	0
0	0	0	0	0	0	0	0	0	0	0	0	0	0	0
0	0	0	0	0	0	0	0	0	0	0	0	0	0	0
0	0	0	0	0	0	0	0	0	0	0	0	0	0	0
0	0	0	0	0	0	0	0	0	0	1	2	3	0	0
0	0	0	0	0	0	0	0	0	0	1	1	0	0	0
0	0	0	0	0	0	0	0	0	0	0	0	0	0	0
0	0	0	0	0	0	0	0	0	0	0	0	0	0	0
0	0	0	0	0	0	0	0	0	0	1	0	0	0	0
0	0	0	0	0	0	0	0	0	0	0	0	2	0	0
0	0	0	0	0	0	0	0	0	0	0	0	0	0	0
0	0	0	0	0	0	0	0	3	0	1	0	0	0	0
0	0	0	0	0	0	0	0	0	0	1	1	0	0	0
0	0	0	0	0	0	0	0	0	0	1	0	0	1	0
0	0	0	0	0	0	0	0	0	0	0	0	0	0	0
0	0	0	0	0	0	0	0	0	0	0	0	0	0	0
27	7	0	0	4	0	4	0	6	3	4	8	11	4	0
0	0	0	0	2	0	0	0	0	0	2	1	1	0	0
0	0	0	0	0	0	0	0	0	0	0	1	0	0	0
0	0	0	0	0	0	0	0	0	0	0	1	0	0	0
0	0	0	0	0	0	0	0	0	0	1	0	0	0	0
0	0	0	0	1	0	0	0	0	0	4	2	3	1	0
12	0	0	2	0	0	0	0	3	24	41	9	7	11	0
0	0	0	0	0	0	0	0	0	0	0	0	0	0	0
0	0	0	0	0	0	0	0	0	0	0	0	2	0	0
0	0	0	0	0	0	0	0	0	0	0	0	0	0	0
0	0	0	0	0	0	0	0	0	0	0	0	1	0	0
0	0	0	0	0	0	0	0	3	2	4	0	0	0	0
0	0	0	0	0	0	0	0	0	0	0	0	0	0	0
0	0	0	0	0	0	0	0	0	0	0	0	0	0	0

0	0	2	0	2	0	0	0	0	0	0	0	0	0	0
0	0	0	0	0	0	0	0	0	1	0	0	0	0	0
0	0	0	0	0	0	0	0	0	0	0	0	0	0	0
0	0	0	0	0	0	0	0	0	3	1	3	2	0	0
0	0	0	0	0	0	0	0	0	2	1	3	1	0	0
1	0	0	0	0	0	0	0	2	0	1	0	0	0	0
1	0	0	4	1	0	1	0	0	0	0	2	6	0	0
5	0	0	5	21	19	2	0	6	3	0	3	0	6	0
2	2	2	19	10	2	6	0	0	3	1	1	0	0	0
0	0	0	0	2	0	1	0	0	2	0	0	0	0	0
0	0	0	0	0	0	0	0	0	0	0	1	0	0	0
0	0	0	0	0	0	0	0	0	1	0	0	0	0	0
0	0	0	0	0	0	0	0	0	0	0	0	0	0	0
0	0	0	0	0	0	0	0	0	1	0	0	0	0	0
5	0	0	0	2	2	2	0	0	8	6	15	15	12	0
1	0	0	0	0	0	1	0	0	1	0	5	0	0	0
0	0	0	0	0	0	0	0	0	0	0	1	0	0	0
0	0	0	0	0	0	0	0	0	0	0	0	1	0	0
0	0	0	0	0	0	0	0	0	0	1	0	0	1	0
0	0	0	0	0	0	0	0	0	0	0	0	0	0	0
0	8	2	20	5	5	2	0	12	10	2	1	1	0	0
0	0	0	0	0	3	0	0	0	0	0	0	1	0	0
0	2	2	4	6	0	0	0	3	2	0	1	0	0	0
1	0	0	0	0	0	0	0	0	0	0	0	1	0	0
0	0	0	0	4	0	0	0	0	1	0	0	0	2	0
0	0	0	0	0	0	0	0	0	0	0	0	0	0	0
0	0	0	0	0	0	0	0	0	2	0	0	0	0	0
0	0	0	0	0	0	0	0	0	0	2	1	0	0	0
0	2	0	0	0	0	0	0	0	0	0	0	0	0	0
0	0	0	0	0	0	0	0	0	0	1	1	0	0	0
0	16	3	24	9	4	0	1	0	0	0	0	0	0	0
0	0	0	0	0	0	0	0	0	0	0	0	0	0	0
0	0	0	0	1	0	0	0	0	0	0	0	0	0	0
0	0	0	0	0	0	0	0	2	0	0	0	0	0	0
0	0	0	0	0	0	0	0	0	0	0	0	0	0	0
0	0	0	0	0	0	0	0	0	0	0	0	0	0	0
1	0	1	0	0	0	0	0	0	0	0	0	1	0	0
4	7	2	7	17	2	0	0	14	0	1	1	0	2	0
0	0	0	0	0	0	0	0	0	0	0	0	0	0	0
6	0	0	0	0	0	0	0	0	0	0	0	0	0	0
0	3	0	0	6	6	4	2	0	13	2	3	1	5	0
0	0	0	0	0	0	0	0	0	0	0	0	0	0	0
0	1	0	0	0	0	0	0	0	0	0	0	0	0	0
0	23	8	32	2	30	1	1	0	1	1	0	1	0	0
0	75	43	65	33	17	3	0	42	7	3	2	8	10	0
0	7	0	0	0	0	0	0	0	0	0	0	0	0	0
8	0	0	0	0	4	0	0	3	2	0	1	0	0	0
0	0	0	0	0	0	0	0	0	1	0	0	1	0	0
94	**153**	**67**	**183**	**135**	**94**	**27**	**4**	**117**	**102**	**113**	**124**	**107**	**85**	**0**

*/**	*/**		**	**			**		*/**	**	**	**	**	
SMB32	SMB36	SMB40	SMB44	SMB48	SMB52	SMB56	SMB58	SMB60	SMB62	SMB64	SMB68	SMB72	SMB74	SMB76
-12.00	-13.00	-14.00	-15.00	-16.00	-17.00	-18.00	-18.50	-19.00	-19.50	-20.00	-21.00	-22.00	-22.50	-23.00
9	5	25	10	50	24	11	8	2	0	3	6	9	10	19
0	0	0	0	0	0	0	0	0	0	0	0	0	2	0
0	0	0	0	0	0	0	0	0	0	0	0	0	0	0
0	0	0	0	0	0	0	0	0	0	0	0	0	0	0
0	0	0	0	0	0	0	0	0	0	0	0	0	0	3
0	0	0	0	2	0	7	0	0	0	1	7	12	1	0
0	0	0	0	0	0	0	0	0	0	0	0	2	0	0
12	0	0	3	4	3	2	0	2	0	1	2	14	10	8
0	0	0	0	0	0	0	0	0	0	0	0	0	0	0
0	0	0	0	0	0	0	4	0	0	0	0	1	0	0
0	0	0	0	0	0	0	0	0	0	0	2	0	0	0
0	0	0	0	0	0	0	0	0	0	0	0	0	0	0
0	0	0	0	0	0	0	0	0	0	0	0	0	0	0
0	0	0	0	0	0	0	0	0	0	0	0	0	0	2
0	0	0	0	0	0	0	0	0	0	0	0	0	0	0
0	0	0	0	0	0	0	0	0	0	0	0	0	0	1
0	0	0	0	0	0	4	0	0	0	0	0	0	0	2
0	0	5	0	0	0	0	0	0	0	0	0	0	0	0
0	0	0	0	0	0	0	0	0	0	0	2	0	0	2
0	0	0	0	0	0	0	0	0	0	0	0	0	0	0
0	0	0	0	0	0	0	0	0	1	0	0	1	2	1
0	0	0	0	0	0	0	0	0	1	0	0	0	0	0
0	0	0	0	0	0	0	0	0	0	0	0	0	0	0
0	0	0	0	0	0	0	0	2	0	0	0	0	0	0
0	0	0	0	0	0	0	0	0	0	0	0	0	0	0
0	0	0	2	0	0	0	0	0	0	0	0	0	0	0
0	0	0	0	0	0	0	0	0	0	0	0	0	1	0
0	0	0	0	0	0	0	0	0	0	0	0	0	0	0
0	0	0	0	6	0	0	0	0	0	0	0	0	1	0
0	0	0	0	0	0	0	0	0	0	0	0	0	0	0
0	0	0	0	0	0	1	0	0	0	0	1	0	0	0
0	0	5	0	0	0	0	0	0	0	0	0	3	0	0
0	0	0	0	0	0	0	0	3	0	0	0	0	3	0
0	0	3	0	9	10	6	0	2	0	2	10	0	0	0
0	0	3	0	0	4	0	0	0	0	0	1	3	0	4
4	0	0	0	2	0	0	0	0	0	0	0	2	1	0
0	0	0	0	0	0	0	0	0	0	0	0	0	0	0
0	0	0	0	0	0	0	0	0	0	0	0	0	0	4
0	0	0	6	2	0	1	0	0	0	0	9	4	16	2
0	4	19	38	19	6	11	0	0	0	0	11	17	24	21
0	0	0	0	0	3	0	0	0	0	0	0	0	0	0
0	0	2	0	0	3	0	0	1	0	0	0	2	3	0
0	0	0	0	0	0	2	2	0	0	0	0	0	0	0
0	0	0	0	0	0	0	0	0	0	0	0	0	0	0
0	0	0	0	0	0	0	0	0	0	0	0	1	0	0
0	0	0	9	2	0	0	0	0	0	0	0	0	0	0
0	0	0	0	0	0	0	6	0	0	0	0	0	0	0

0	0	0	0	0	0	0	2	0	1	5	0	0	0	0
0	0	0	0	0	0	0	0	1	0	0	0	0	0	0
0	0	0	0	0	0	0	0	0	0	0	0	0	0	0
0	0	3	0	0	0	0	0	0	0	0	0	0	0	8
0	0	0	3	0	0	7	3	0	0	0	0	0	0	2
0	0	0	0	0	0	0	0	0	0	0	0	0	0	0
2	0	0	0	0	0	0	0	0	0	1	1	3	4	0
0	0	0	9	16	11	0	2	2	0	1	7	10	0	4
0	0	0	0	8	0	2	2	0	0	0	0	0	1	1
0	0	0	0	0	0	0	0	0	0	1	0	0	1	0
0	0	0	0	0	0	0	0	0	0	0	0	0	0	0
0	0	22	0	0	0	0	0	0	0	0	0	4	8	8
0	0	9	0	0	0	0	0	0	0	0	0	0	0	0
0	0	0	0	0	0	0	0	0	0	0	0	0	0	0
0	0	3	12	0	4	2	0	0	0	2	4	12	21	12
0	0	2	3	1	2	0	0	0	0	0	0	1	5	1
0	0	0	0	0	0	0	0	0	0	0	0	0	0	0
0	0	0	0	0	0	0	0	0	0	0	0	0	0	0
0	0	0	0	0	0	0	0	1	0	0	0	2	0	0
0	0	0	0	0	0	0	0	0	0	0	0	0	0	0
0	0	0	0	0	5	0	2	0	3	0	0	0	0	5
0	0	3	0	0	0	4	22	16	0	3	11	0	0	3
0	0	0	0	0	0	0	0	0	0	0	0	0	2	0
0	0	0	0	0	0	0	0	0	0	0	0	0	0	0
0	0	0	0	0	2	0	0	0	4	0	0	0	0	2
0	0	0	0	0	0	4	0	0	0	0	0	0	0	0
0	0	0	0	0	0	0	0	0	0	0	0	0	0	0
0	0	0	0	0	0	2	16	19	0	0	0	0	2	0
0	0	0	0	0	0	10	0	10	0	0	0	0	0	0
0	0	0	0	0	0	0	0	0	0	0	1	0	0	0
0	0	0	0	2	3	15	0	20	0	1	0	0	0	0
0	0	0	0	0	0	0	0	0	0	0	0	0	0	0
0	0	0	0	0	0	0	0	0	0	0	0	0	0	0
0	0	0	0	0	0	0	0	0	0	0	0	0	0	0
0	0	0	0	0	3	0	0	0	0	0	0	0	0	0
0	0	0	0	3	0	0	0	0	0	0	0	0	0	0
0	0	0	0	0	0	0	0	0	0	0	0	0	0	0
0	0	0	3	11	2	0	6	16	4	1	4	8	3	0
0	0	0	0	0	0	0	2	0	1	0	2	0	0	0
0	0	0	0	0	0	0	0	0	0	0	0	0	0	0
0	0	0	0	3	0	0	0	0	1	0	7	8	6	0
0	0	0	0	0	1	0	0	0	0	0	0	0	0	0
0	0	0	0	1	0	0	0	4	0	0	3	0	1	0
0	0	16	0	0	5	0	19	18	1	3	32	0	0	0
5	0	12	4	4	11	20	8	33	0	5	22	5	8	11
0	0	0	0	0	0	0	0	0	1	0	0	0	0	0
0	0	0	0	0	1	0	0	0	1	3	0	0	0	0
0	0	0	0	0	0	0	0	0	0	0	0	0	0	0
32	**9**	**132**	**102**	**145**	**103**	**111**	**104**	**152**	**19**	**33**	**145**	**124**	**136**	**126**